



HAL
open science

Tudor-SN Promotes Early Replication of Dengue Virus in the *Aedes aegypti* Midgut

Sarah H el ene Merklings, Vincent Raquin, St ephanie Dabo, Annabelle
Henrion-Lacritick, Herv e Blanc, Isabelle Moltini-Conclois, Lionel Frangeul,
Hugo Varet, Maria-Carla P Saleh, Louis Lambrechts

► **To cite this version:**

Sarah H el ene Merklings, Vincent Raquin, St ephanie Dabo, Annabelle Henrion-Lacritick, Herv e Blanc,
et al.. Tudor-SN Promotes Early Replication of Dengue Virus in the *Aedes aegypti* Midgut. *iScience*,
2020, 23 (2), pp.100870. 10.1016/j.isci.2020.100870 . pasteur-02562446

HAL Id: pasteur-02562446

<https://pasteur.hal.science/pasteur-02562446>

Submitted on 4 May 2020

HAL is a multi-disciplinary open access archive for the deposit and dissemination of scientific research documents, whether they are published or not. The documents may come from teaching and research institutions in France or abroad, or from public or private research centers.

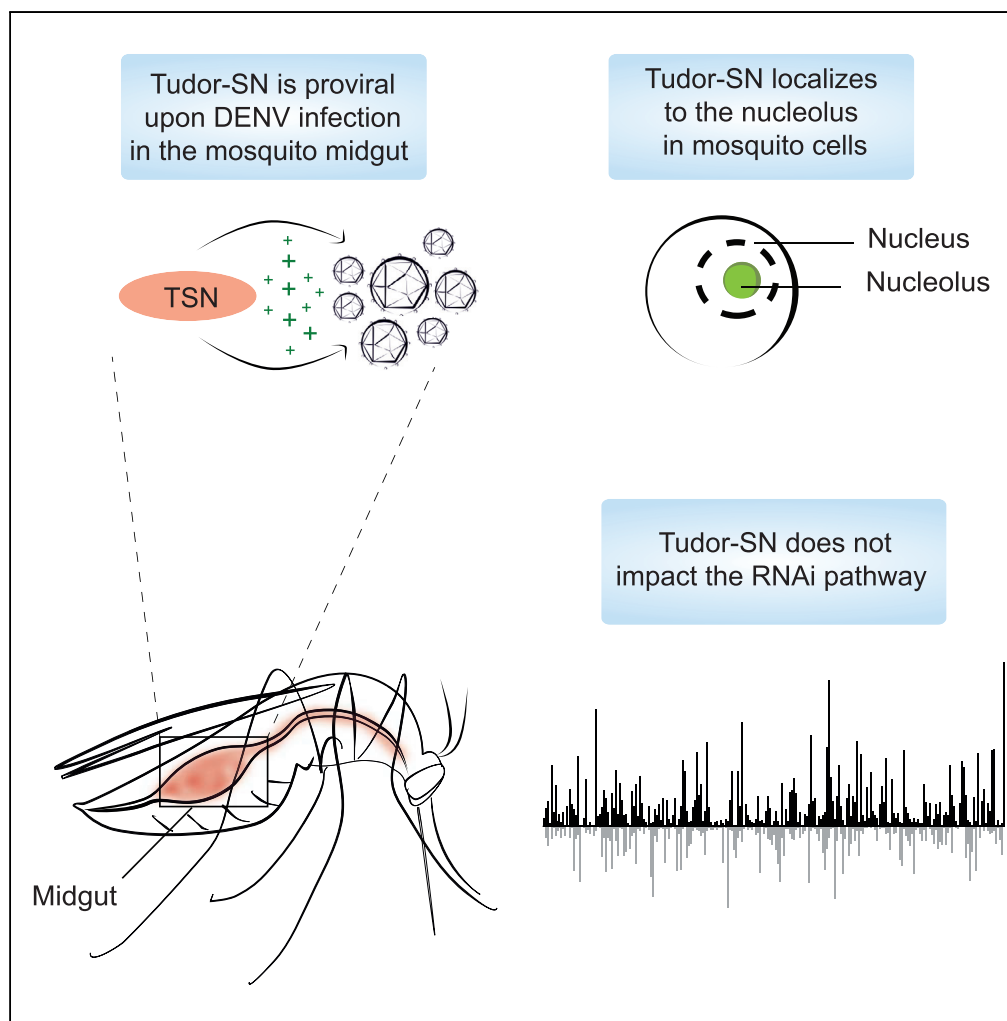
L'archive ouverte pluridisciplinaire **HAL**, est destin ee au d ep ot et  a la diffusion de documents scientifiques de niveau recherche, publi es ou non,  emanant des  tablissements d'enseignement et de recherche fran ais ou  trangers, des laboratoires publics ou priv es.



Distributed under a Creative Commons Attribution - NonCommercial - NoDerivatives 4.0
International License

Article

Tudor-SN Promotes Early Replication of Dengue Virus in the *Aedes aegypti* Midgut



Sarah H el ene Merkle, Vincent Raquin, St ephane Dabo, ..., Hugo Varet, Maria-Carla Saleh, Louis Lambrechts

carla.saleh@pasteur.fr (M.-C.S.)
louis.lambrechts@pasteur.fr (L.L.)

HIGHLIGHTS

Tudor-SN is upregulated in the *Ae. aegypti* midgut early upon dengue virus infection

Tudor-SN promotes viral replication *in vitro* and *in vivo*

Tudor-SN localizes to the nucleolus in mosquito cells

Tudor-SN is not required for RNAi function *in vivo*

Merkling et al., iScience 23, 100870
February 21, 2020   2020 The Author(s).
<https://doi.org/10.1016/j.isci.2020.100870>

Article

Tudor-SN Promotes Early Replication of Dengue Virus in the *Aedes aegypti* Midgut

Sarah H el ene Merklings,¹ Vincent Raquin,^{1,5,6} St ephanie Dabo,¹ Annabelle Henrion-Lacritick,² Herv e Blanc,² Isabelle Moltini-Conclois,¹ Lionel Frangeul,² Hugo Varet,^{3,4} Maria-Carla Saleh,^{2,*} and Louis Lambrechts^{1,7,*}

SUMMARY

Diseases caused by mosquito-borne viruses have been on the rise for the last decades, and novel methods aiming to use laboratory-engineered mosquitoes that are incapable of carrying viruses have been developed to reduce pathogen transmission. This has stimulated efforts to identify optimal target genes that are naturally involved in mosquito antiviral defenses or required for viral replication. Here, we investigated the role of a member of the Tudor protein family, Tudor-SN, upon dengue virus infection in the mosquito *Aedes aegypti*. Tudor-SN knockdown reduced dengue virus replication in the midgut of *Ae. aegypti* females. In immunofluorescence assays, Tudor-SN localized to the nucleolus in both *Ae. aegypti* and *Aedes albopictus* cells. A reporter assay and small RNA profiling demonstrated that Tudor-SN was not required for RNA interference function *in vivo*. Collectively, these results defined a novel proviral role for Tudor-SN upon early dengue virus infection of the *Ae. aegypti* midgut.

INTRODUCTION

The mosquito *Aedes aegypti* transmits a wide range of pathogens to humans, many with severe consequences on public health, including dengue, Zika, and chikungunya viruses (Gould et al., 2017). For instance, dengue virus (DENV) infects 390 million people annually (Bhatt et al., 2013) and 50% of the world's population is at risk for infection (Brady et al., 2012). DENV belongs to the *Flaviviridae* family and has a positive-sense, single-stranded RNA genome. DENV exists as four genetic types (DENV-1, -2, -3 and 4) that are phylogenetically related and loosely antigenically distinct (Katzelnick et al., 2015). In the wild, mosquitoes acquire DENV by feeding on a viremic host. After the infectious blood meal, DENV infection is first established in the mosquito midgut before spreading systematically and reaching the salivary glands, where the virus engages in further replication (Raquin and Lambrechts, 2017) before being transmitted to the next host via the saliva released during the bite (Salazar et al., 2007; Black et al., 2002).

The primary prevention strategy against arboviral diseases relies on the control of vector populations. Current vector control methods are mainly based on insecticides. Despite having been applied for decades, the burden of arboviral diseases keeps increasing (Messina et al., 2019). Human travel, urbanization, climate change, and geographic expansion of mosquito vectors increase pathogen transmission and spread (Weaver, 2013). Over the last two decades, research efforts have led to the production of laboratory-engineered mosquitoes that either suppress wild vector populations or render them incapable of transmitting pathogens (Champer et al., 2016; Yakob et al., 2017). As the methods for genetic modification of mosquitoes develop, the need to identify optimal target genes that are naturally involved in mosquito antiviral defenses or required for viral replication also increases. Preferably, such pro- or antiviral target genes would act early during the course of an infection, and, when engineered, would permit early blocking of virus replication, at the level of the midgut cells. This would hinder viral dissemination and make further transmission of the virus impossible.

The majority of our knowledge about insect antiviral immunity originates from investigations in the model organism *Drosophila melanogaster* (Merklings and Van Rij, 2013; Mongelli and Saleh, 2016), whereas studies in mosquito vectors remain more limited (Bartholomay and Michel, 2018; Simoes et al., 2018; Lee et al., 2019). The Toll, IMD, and Jak-Stat pathways have been implicated in insect innate immune responses to bacteria, fungi, viruses, and parasites. Their activation triggers translocations of NF- B-like or Stat transcription factors to the nucleus, inducing the expression of an array of immune genes encoding antimicrobial peptides and virus restriction factors, among others (Bartholomay and Michel, 2018; Simoes et al., 2018; Lee et al., 2019; Merklings and Van Rij, 2013; Mongelli and Saleh, 2016). Another major branch of insect

¹Institut Pasteur, Insect-Virus Interactions Unit, UMR2000, CNRS, 75015 Paris, France

²Institut Pasteur, Viruses and RNA Interference Unit, UMR3569, CNRS, 75015 Paris, France

³Hub de Bioinformatique et Biostatistique – D epartement Biologie Computationnelle, Institut Pasteur, USR 3756, CNRS, Paris, France

⁴Plate-forme Technologique Biomics – Centre de Ressources et Recherches Technologiques (C2RT), Institut Pasteur, Paris, France

⁵Present address: UMR754, Universit e Claude Bernard Lyon 1, Institut National de la Recherche Agronomique, Ecole Pratique des Hautes Etudes, SFR BioSciences Gerland, Lyon, France

⁶Present address: Universit e de Lyon, Ecologie microbienne, UMR CNRS 5557, UMR INRA 1418, VetAgro Sup, Universit e Lyon 1, Villeurbanne, France

⁷Lead Contact

*Correspondence: carla.saleh@pasteur.fr (M.-C.S.), louis.lambrechts@pasteur.fr (L.L.)

<https://doi.org/10.1016/j.isci.2020.100870>



innate immunity is RNA interference (RNAi), which encompasses several pathways leading to the production of small RNA molecules of different characteristics, such as small interfering RNAs (siRNAs), microRNAs (miRNAs), and P element-induced wimpy testis (PIWI)-interacting RNAs (piRNAs) (Miesen et al., 2016). The siRNA pathway is hitherto considered as the cornerstone of antiviral immunity in insects. It is initiated with the sensing and cleavage of viral double-stranded RNA (dsRNA) into 21-nucleotide-long siRNAs by the endonuclease Dicer-2. These siRNAs are loaded in the RNA-induced silencing complex (RISC) that guides Ago2-mediated cleavage of viral target sequences (Miesen et al., 2016). Numerous studies reported that depletion of siRNA pathway components in mosquitoes resulted in increased arbovirus replication (Campbell et al., 2008; Keene et al., 2004; Myles et al., 2008; Sanchez-Vargas et al., 2009; Franz et al., 2006).

Although several pathways involved in antiviral immunity have been characterized in mosquitoes, several aspects of anti-DENV defense remain elusive. For example, the siRNA pathway was shown to inefficiently restrict DENV replication in the *Ae. aegypti* midgut (Olmo et al., 2018). Besides, most of previous studies have focused on mosquito antiviral or restriction factors that antagonize DENV, but little is known about mosquito host factors with a proviral function, that is, factors enhancing DENV propagation. Several human factors required for DENV infectivity were recently discovered through genome-wide CRISPR screens (Savidis et al., 2016; Zhang et al., 2016; Marceau et al., 2016), whereas only a handful of DENV host factors have been identified in mosquitoes to date (Londono-Renteria et al., 2015; Jupatanakul et al., 2014; Sessions et al., 2009; Raquin et al., 2017). Although CRISPR screens cannot be readily carried out in live mosquitoes, transcriptome analysis by high-throughput RNA sequencing is a powerful method to identify DENV host and restriction factors *in vivo* (Sigle and McGraw, 2019). For example, novel DENV restriction factors (DVRF-1 and -2) that depend on the Jak-Stat pathway activation have been uncovered by overlapping transcriptional profiles of mosquitoes infected with DENV and mosquitoes with a hyperactive Jak-Stat pathway (Souza-Neto et al., 2009).

In this study, we exploited a unique transcriptomic dataset that we previously generated by performing RNA sequencing on individual midguts in a field-derived *Ae. aegypti* population during early DENV-1 infection (Raquin et al., 2017). In addition to a conventional pairwise comparison of gene expression between DENV-infected and uninfected controls, we also used an approach to detect correlations between viral RNA load and gene expression. Of 269 candidate genes identified by either method, only four were differentially expressed upon DENV-1 infection and had expression levels that correlated with viral RNA load in infected mosquitoes (Raquin et al., 2017). Among the four candidate genes identified by both methods was a gene encoding a member of the Tudor protein family, Tudor Staphylococcal Nuclease (abbreviated Tudor-SN or TSN), which we selected for further investigation in the present study. Using RNAi-mediated gene knockdown *in vivo*, we found that reduced TSN expression resulted in lower viral loads *in vitro* and *in vivo*. Immunofluorescence assays revealed that TSN localized to the nucleolus and did not colocalize to DENV replication sites in DENV-infected cells. Finally, we used a reporter assay and small RNA profiling to show that TSN was not involved in RNAi function in the midgut of adult mosquitoes. Altogether, our results demonstrate that TSN has an early proviral effect on DENV replication in the midgut and could be considered as a target to develop genetically modified mosquitoes that are refractory to DENV infection.

RESULTS

TSN Expression Is Upregulated upon DENV-1 Infection and Positively Correlates with Viral Loads

Our previous transcriptomic analysis revealed that TSN (AAEL000293) expression was significantly upregulated upon DENV-1 infection relative to mock controls 1 day after exposure to the infectious blood meal (Figure 1A) but not 4 days post blood meal (Figure 1B). Inversely, we found that TSN expression was not significantly correlated with DENV-1 viral loads 1 day post blood meal (Figure 1C) but was positively correlated with DENV-1 RNA loads 4 days post blood meal (Figure 1D). Thus, we concluded that TSN expression was induced by DENV-1 infection within 24 h after the infectious blood meal and that subsequently, its expression was positively correlated with DENV-1 replication. The positive correlation was suggestive of a proviral role for TSN upon DENV-1 infection.

TSN Is a DENV Proviral Factor *In Vitro*

First, we sought to test the proviral role of TSN *in vitro* by using *Ae. aegypti* Aag2 cells in culture. We transfected Aag2 cells with dsRNA to trigger RNAi-mediated knockdown of TSN or an exogenous green

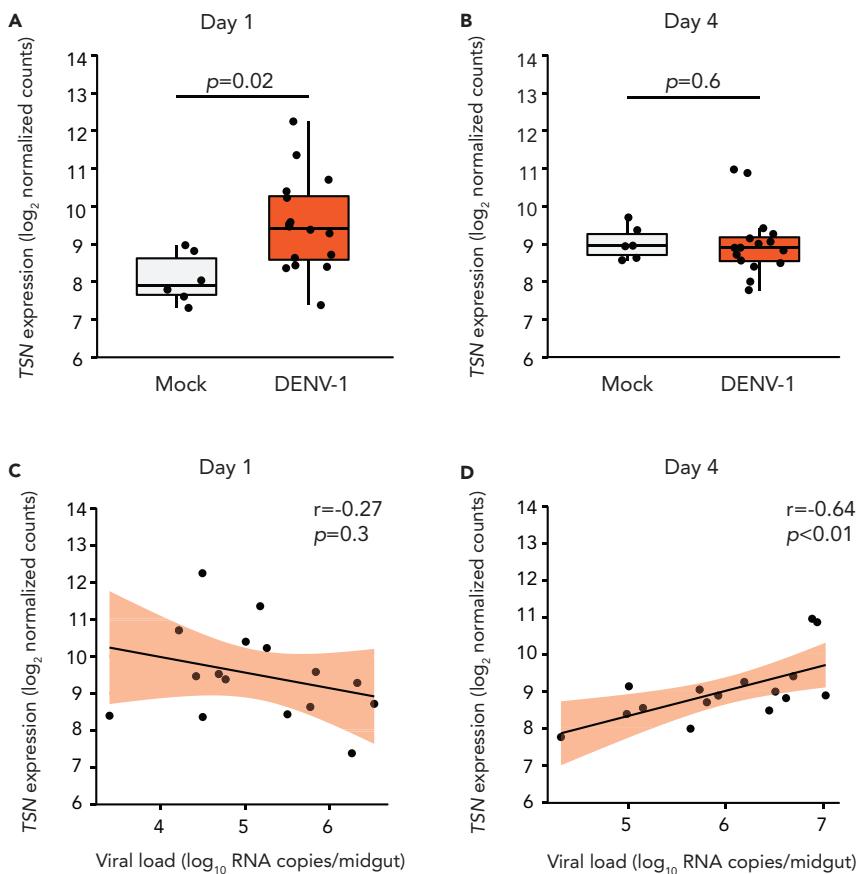


Figure 1. TSN Is Upregulated upon DENV-1 Infection and Correlates Positively with Midgut Viral Loads

(A and B) TSN midgut expression levels on day 1 and day 4 post DENV-1 exposure. Log₂-transformed TSN normalized RNA-seq counts are shown in mock-infected (n = 6) and DENV-1-infected (n = 16) midguts. p values of the pairwise t tests are indicated.

(C and D) Correlation of TSN expression level and viral load in DENV-1-infected midguts on day 1 and day 4 post virus exposure. Log₂-transformed TSN normalized RNA-seq counts are shown as a function of the log₁₀-transformed midgut viral load. Black lines represent the linear regression and light purple shaded areas represent the 95% confidence intervals of the regression. Pearson's coefficients of determination (r) and p values of the linear regression coefficient are indicated.

fluorescent protein (GFP) sequence (Table 1) and subsequently inoculated them with DENV-1 at a multiplicity of infection of 1. We measured TSN expression levels by reverse transcription quantitative PCR (RT-qPCR) at 0, 12, 24, 36, 48, 72 and 96 h post infection and found that TSN knockdown efficiency ranged from ~50% to 80% and was statistically significant at most of the time points (Figure 2A). We visualized TSN protein levels by western blotting using an antibody directed against the human ortholog of TSN named SND1, which also reacted against the *Ae. aegypti* TSN. We confirmed that TSN knockdown reduced TSN protein levels by 70%–80% in Aag2 cells at 24 and 48 h post DENV-1 infection, compared with the GFP control (Figure 2B). To determine whether TSN also augmented viral infection *in vitro*, we measured both DENV-1 RNA levels (Figure 2C) and DENV-1 infectious titers by focus-forming assay (Figure 2D) over the course of infection. We found that DENV-1 RNA levels were significantly reduced upon TSN knockdown relative to control levels at 24 h post infection (Figure 2C, $p < 0.01$). Moreover, DENV-1 RNA levels were consistently lower in TSN-depleted cells from 24 to 96 h post infection. DENV-1 infectious titers were also significantly reduced upon TSN knockdown at 24 and 48 h post infection (Figure 2D, $p < 0.05$ and $p < 0.001$, respectively). Overall, these data demonstrated a proviral role of TSN *in vitro*.

TSN Is a DENV Proviral Factor *In Vivo*

To confirm the proviral role of TSN *in vivo*, we experimentally reduced TSN expression in adult female mosquitoes by intrathoracic injection of dsRNA and subsequently exposed them to an infectious blood

Organism	Primer/Probe ^a	Sequence (5'-3')	Product Size (bp)	Reference
<i>Ae. aegypti</i>	rp49-F	ACAAGCTTGCCCCCAACT	97	(Gentile et al., 2005)
	rp49-R	CCGTAACCGATGTTTGCC		
	TSN-F	CTGCAGATGAACGTCGAGTA	100	This study
	TSN-R	CATCGCTGACCAGTTCCTT		
	dsTSN-F ^b	taatacgactcactatagggAAAGGCCAAATGGAGCGACT	312	This study
	dsTSN-R ^b	taatacgactcactatagggGACGTCACGTTGCAGCAG		
	dsGFP-F ^b	taatacgactcactatagggATGGTGAGCAAGGGCGAG	501	This study
	dsGFP-R ^b	taatacgactcactatagggTTACTTGTACAGCTCGTC		
	dsLuc-F ^b	taatacgactcactatagggCGCCCTGGTTCCTGGAAC	556	This study
	dsLuc-R ^b	taatacgactcactatagggAGAATCTCACGCAGGCAGTTC		
DENV-1	NS5-F	GGAAGGAGAAGGACTCCACA	105	(Fontaine et al., 2016)
	NS5-R	ATCCTTGTATCCCATCCGGCT		
	NS5-Probe	CTCAGAGACATATCAAAGATTCCAGGG		
DENV-3	NS5-F	AGAAGGAGAAGGACTGCACA	105	This study
	NS5-R	ATTCTTGTGTCCCAACCGGCT		
CHIKV	CHIK_10366_F	AAGCTCCGCGTYCTTTACCAAG	208	(Modified from Pastorino et al., 2005)
	CHIK_10574_R	CCAAATTGTCCYGGTCTTCTT		

Table 1. List of Oligonucleotide Primers and Molecular Probes Used in This Study

^aF stands for forward and R stands for reverse.

^bT7 sequences are written in bold.

meal containing 10^7 focus-forming units (FFU)/mL of DENV-1 (Figure 3A). First, we monitored *TSN* expression levels in individual mosquitoes by RT-qPCR on days 0, 1, and 4 after the infectious blood meal. On day 0, which corresponds to 3 days after injection of dsTSN, *TSN* expression was significantly knocked down relative to mosquitoes injected with a control dsRNA targeting *GFP* (Figure 3B, $p < 0.001$). Reduced *TSN* expression persisted over time through day 1 (Figure 3C, $p < 0.0001$) and day 4 (Figure 3D, $p = 0.01$) after exposure to the infectious blood meal. Importantly, reduced *TSN* expression did not significantly impact the survival of mosquitoes during the seven days following injection compared with the dsGFP control (Figure 3E, $p = 0.54$). We also measured *TSN* expression in head, thorax, abdomen, ovary, and midgut tissues in sugar-fed or blood-fed mosquitoes and found that *TSN* expression was significantly upregulated in midguts 1 day after a blood meal, suggesting a tissue-specific role within the first day after a blood meal (Figures S1A and S1B, related to Figure 3). Next, we measured DENV-1 RNA loads by RT-qPCR and found an ~50% reduction of viral loads in mosquito midguts depleted for *TSN*, compared with the GFP control, 4 days after the infectious blood meal (Figure 3F, $p < 0.0001$). We also measured DENV-1 RNA loads one day after the infectious blood meal and did not observe a decrease of viral loads. However, this is most likely due to the presence of viral RNA in the undigested blood still present in the midgut at this time point, as shown in a previous report (Raquin et al., 2017). These results confirmed the proviral role of *TSN* during DENV-1 infection in the mosquito midgut 4 days after the infectious blood meal. However, we found no evidence that *TSN* knockdown had an impact on infection prevalence after DENV-1 exposure. Among the mosquito midguts analyzed by RT-PCR on day 4, we found that 88% and 90% were positive for DENV-1 RNA in the *TSN* knockdown and the dsGFP control groups, respectively (Figure 3G, $p = 0.59$). In addition to DENV-1, we assessed the proviral role of *TSN* upon infection by another DENV serotype, DENV-3, and the alphavirus chikungunya virus (CHIKV). We injected adult mosquitoes with dsRNA against *TSN* or *luciferase* as a negative control and offered them an infectious blood meal 3 days later. We confirmed *TSN* knockdown (Figures S2A, related to Figure 3) and observed a significant reduction in DENV-3 RNA levels in individual mosquito midguts (Figures S2B, related to Figure 3) 4 days post DENV-3 exposure. We confirmed *TSN* knockdown 2 and 4 days post CHIKV exposure (Figures S2C and S2E,

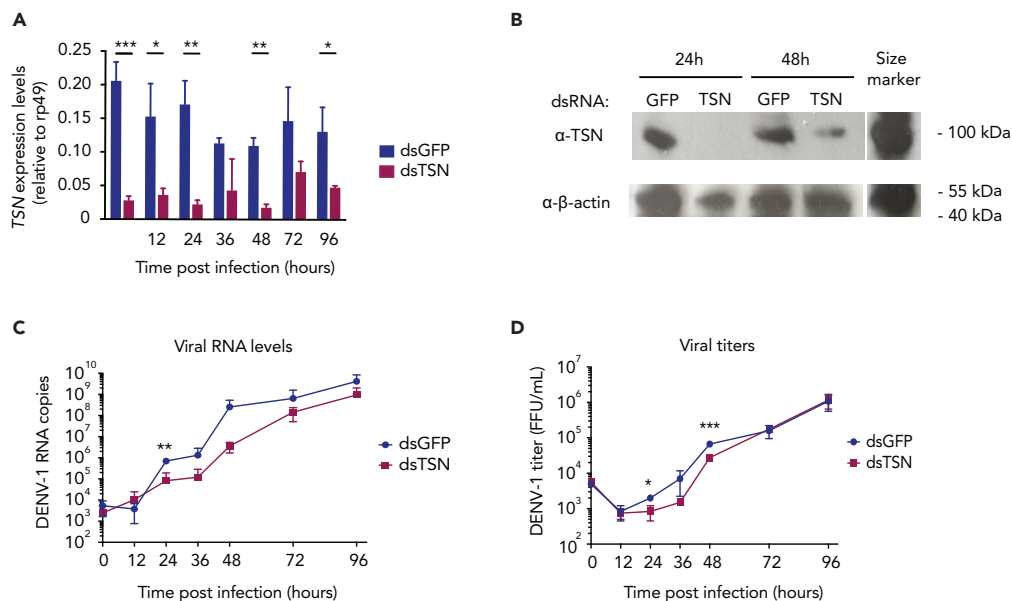


Figure 2. TSN Promotes DENV-1 Infection in *Ae. aegypti* Aag2 Cells

(A) TSN expression levels in Aag2 cells transfected with dsRNA targeting *TSN* (dsTSN) or *GFP* (dsGFP), over the course of DENV-1 infection at a multiplicity of infection of 0.1. Aag2 cells were transfected 3 and 1 day prior to virus infection. TSN expression was measured by RT-qPCR and normalized to *rp49*. Data represent mean and standard deviation of three biological replicates. * $p < 0.05$; ** $p < 0.01$; *** $p < 0.001$ (Student's *t* test). Data are from the same experiment shown in (C) and (D).

(B) Western blot analysis of TSN expression in Aag2 cells 24 and 48 h after viral infection. An anti- β -actin monoclonal antibody was used for loading control. Molecular mass in expressed in kilodaltons (kDa).

(C and D) Analysis of DENV-1 RNA levels (C) or DENV-1 infectious titers (D) over the course of DENV-1 infection following TSN or *GFP* knockdown. RNA levels were measured by RT-qPCR on RNA from cell extracts, and infectious titers were determined by focus-forming assay on cell culture supernatants. Data represent mean and standard deviation of three biological replicates. * $p < 0.05$; ** $p < 0.01$; *** $p < 0.001$ (Student's *t* test).

related to Figure 3), but despite a slight reduction of CHIKV RNA levels at both time points the difference with controls was not statistically significant (Figures S2D and S2F, related to Figure 3). Therefore, we found that TSN acted as a proviral factor for two DENV types, DENV-1 and DENV-3, but not for the alphavirus CHIKV. Overall, our data demonstrated that, although TSN does not influence the probability of DENV infection, it promotes early DENV replication in the mosquito midgut.

TSN Localizes to the Nucleolus in Mosquito Cells

It was previously shown that TSN could interact with DENV RNA in mammalian cells (Lei et al., 2011), which led us to ask whether TSN co-localized with DENV-derived RNA in mosquito cells. Double-stranded RNA is produced during the replication of single-stranded RNA viruses like DENV and is a hallmark of RNA virus infection (Weber et al., 2006). Previous reports demonstrated that antibodies directed against dsRNA did not cross-react with cellular rRNA or tRNA and could be used to identify flavivirus replication complexes in infected cells (Emara and Brinton, 2007). To determine the subcellular localization of TSN, we performed immunofluorescence assays in mosquito cells derived from *Ae. albopictus* (C6/36, Figure 4A) or *Ae. aegypti* (Aag2, Figure 4B) using the anti-SDN1 antibody previously validated by western blotting (Figure 3B) and a monoclonal antibody targeting dsRNA (called α K1). In both cell types, we found that TSN was expressed and localized to the nucleolus. Indeed, it localized to the nucleus region but did not overlap with DAPI staining, which is reported to exclude the nucleolus (Sirri et al., 2008). Moreover, the staining was more intense at the nucleus-nucleolus interface where it formed a "ring." TSN localization did not change upon DENV-1 infection, nor did its expression level. Six days after DENV-1 infection of C6/36 and Aag2 cells, dsRNA staining was readily detectable and mainly localized to cytoplasmic regions of infected cells, likely corresponding to viral replication sites. Since TSN localized to the nucleolus, and the dsRNA to the cytoplasm, we did not observe overlapping signals between both stainings. Thus, we conclude that TSN

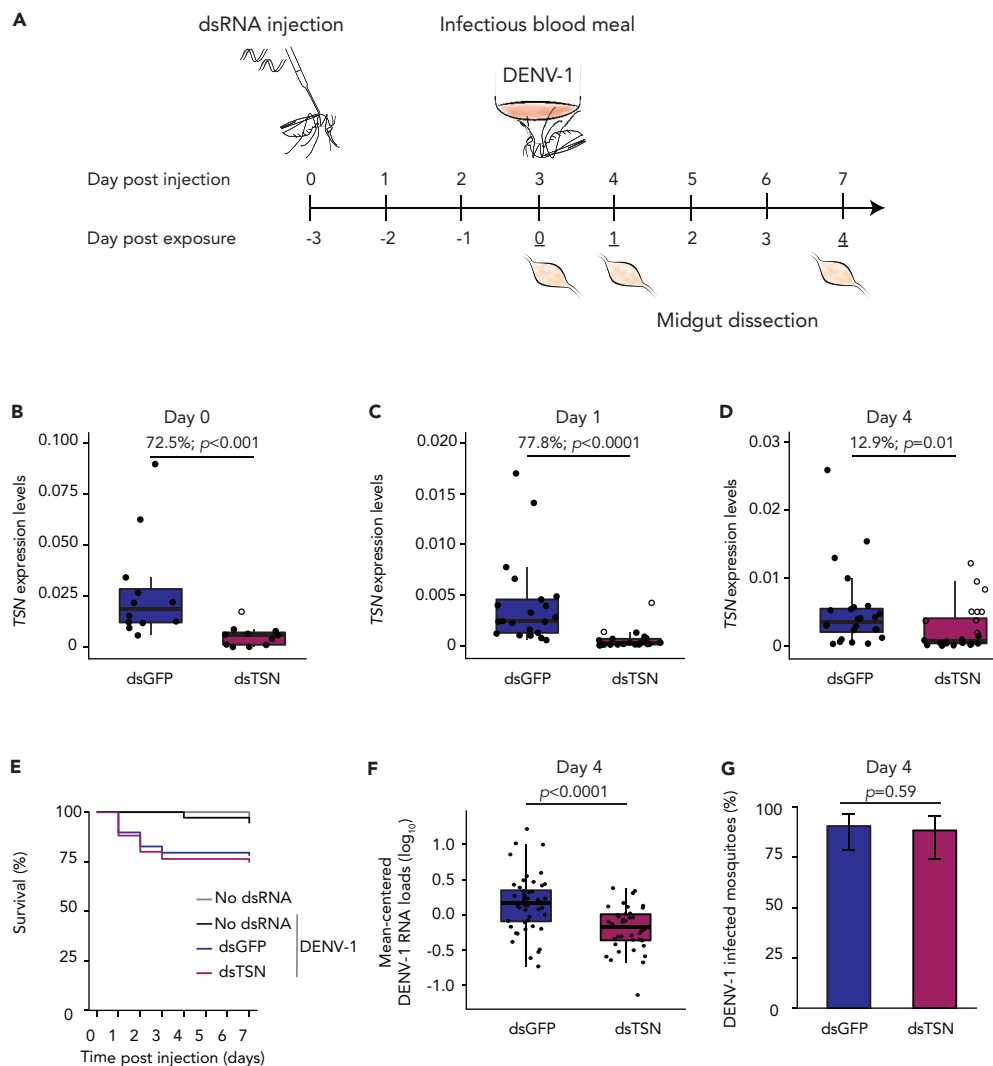


Figure 3. TSN Promotes DENV-1 Infection in the Mosquito Midgut

(A) Experimental scheme of the gene-silencing assays *in vivo*.

(B–D) TSN expression levels following gene knockdown on day 0 (B), day 1 (C), and day 4 (D) after exposure to DENV-1 infectious blood meal. Mean percentage of gene expression knockdown on day 0 (B), day 1 (C), and day 4 (D) after DENV-1 exposure are indicated. Boxplots show TSN expression normalized by *rp49* and expressed as $2^{-\Delta\Delta Ct}$ values in $n = 12$ –24 individual mosquito midguts per group. Individuals with less than 50% gene expression knockdown are shown as empty dots. Data are representative of three separate experiments. *p* values above the graph indicate statistical significance assessed with a Wilcoxon test.

(E) Percentage of survival following dsRNA injection and/or DENV-1 exposure. Mosquitoes were injected with dsRNA targeting TSN ($n = 127$), targeting GFP (dsGFP, $n = 110$) 3 days prior to DENV-1 exposure. Non-injected mosquitoes that fed on an infectious ($n = 71$) or a non-infectious blood meal ($n = 62$) were used as controls. No significant difference in mortality was detected between dsGFP and dsTSN mosquitoes according to a Cox model ($p = 0.54$).

(F) DENV-1 RNA levels in mosquito midguts dissected from mosquitoes previously injected with dsGFP ($n = 53$) or dsTSN ($n = 55$). Boxplots represent the viral load measured by RT-qPCR on day 4 post exposure. Data represent three separate experiments combined. The negative effect of TSN knockdown on viral load was statistically significant in each of the three experiments. Viral loads are adjusted for differences between experiments and expressed in mean-centered DENV-1 RNA loads. The *p* value above the graph indicates statistical significance of the treatment effect assessed with an analysis of variance accounting for the experiment effect.

(G) DENV-1 infection prevalence in mosquito midguts measured by RT-qPCR on day 4 post virus exposure following injection with dsGFP ($n = 53$) and dsTSN ($n = 43$). Data from three separate experiments were combined after verifying the lack of a detectable experiment effect. Error bars represent 95% confidence intervals of the percentages. The *p* value above the graph indicates statistical significance of the treatment effect assessed with a logistic regression.

See also Figures S1 and S2.

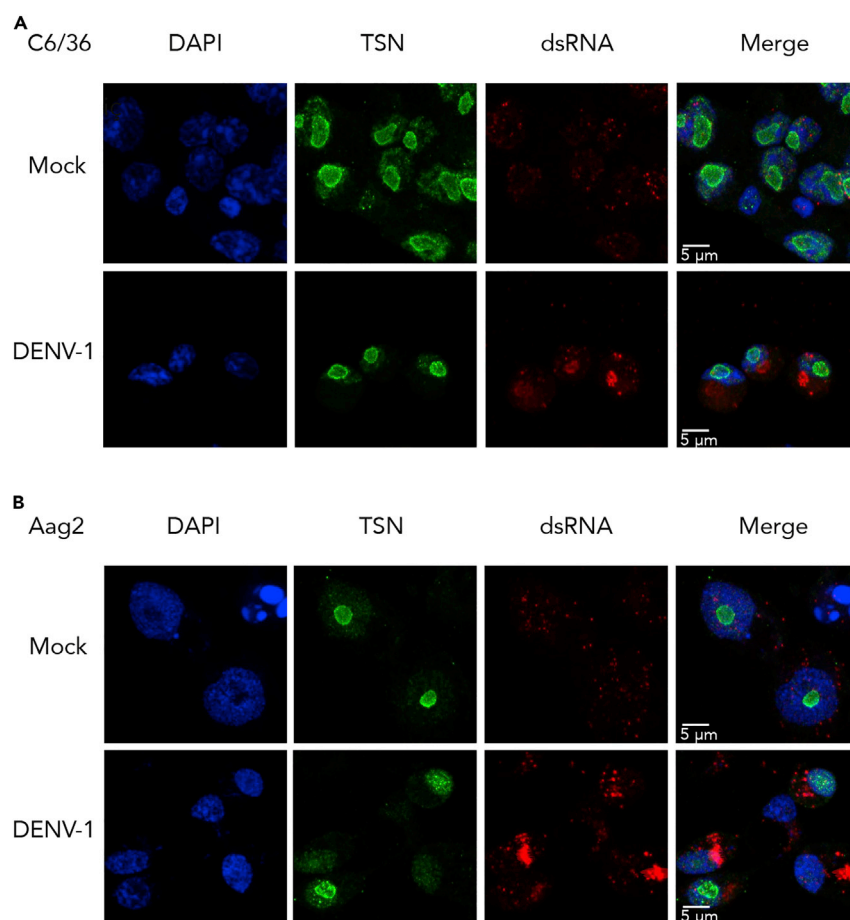


Figure 4. TSN Localizes to the Nucleolus in *Ae. aegypti* and *Ae. albopictus* Cells

(A and B) Immunofluorescence assays in *Ae. albopictus* C6/36 (A) or *Ae. aegypti* Aag2 (B) cells 6 days after infection with DENV-1. Cells were stained with the nuclear stain DAPI, an antibody against TSN coupled to an Alexa 488 secondary fluorescent antibody, and an antibody against dsRNA (α K1) coupled to an Alexa 689 secondary fluorescent antibody. Cells were imaged on a confocal microscope at 63 \times magnification.

does not interact with DENV-1 RNA at its replication site. However, it remains possible that interactions occur with other forms of DENV-1 RNA (positive or negative single-stranded RNA) or viral proteins.

RNAi Is Functional in TSN-Depleted Mosquitoes

Proteins containing Tudor motifs have been implicated in multiple aspects of RNA metabolism such as RNA splicing or small RNA pathways (Lasko, 2010; Siomi et al., 2010). TSN was shown to be a component of the RISC in *Caenorhabditis elegans*, *Drosophila*, and mammals (Caudy et al., 2003) and was suggested to participate in RNAi function in the tick *Ixodes scapularis* (Ayllon et al., 2015). Therefore, we asked whether TSN was involved in RNAi function in *Ae. aegypti*. We adapted a luciferase-based RNAi sensor assay developed in *Drosophila* to mosquitoes (Merklings et al., 2015a, 2015b, Van Cleef et al., 2011). Adult females were intrathoracically injected with a mix of lipofectant along with Firefly luciferase reporter plasmid with Firefly luciferase-specific dsRNA and dsRNA targeting GFP (as a negative control), Ago2 (as a positive control), or TSN (Figure 5A). A reporter plasmid encoding a Renilla luciferase was used as an *in vivo* transfection control. Three days after injection, the efficiency of Firefly luciferase silencing was measured in whole-mosquito homogenates (Figure 5B). When reporter plasmids were injected together with control dsGFP, we observed a wide range of luminescence counts (likely due to variable *in vivo* transfection efficiency), but the average luciferase activity was about 100-fold higher than when dsRNA targeting Firefly luciferase (dsLuc) was co-transfected with the reporter plasmids and control dsGFP. The silencing of Firefly luciferase was partially restored upon knockdown of Ago2, a key gene of the RNAi pathway, demonstrating the

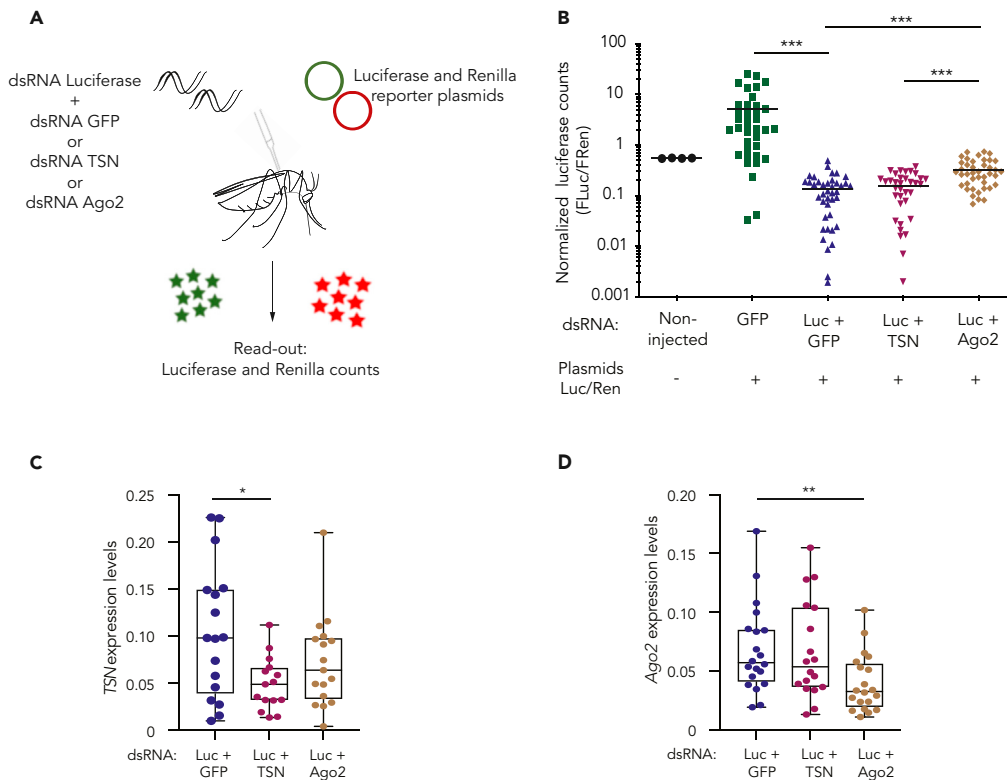


Figure 5. TSN Does Not Enhance RNAi Function

(A) Experimental scheme. Adult mosquitoes were co-injected with Firefly *luciferase* (Fluc) and Renilla *luciferase* (Rluc) reporter plasmids, and dsRNA targeting Fluc in combination with dsRNA against GFP, TSN or Ago2. Luminescence was measured 3 days post injection.

(B) *In vivo* RNAi reporter assay. Reporter gene activity was measured in individual mosquitoes. Luminescence counts of Firefly *luciferase* were normalized to the Renilla *luciferase* counts. Mean and standard deviation are shown. * $p < 0.05$; ** $p < 0.01$; *** $p < 0.001$ (Mann-Whitney t test).

(C and D) Expression levels of *TSN* (C) and *Ago2* (D) measured by RT-qPCR on mosquitoes harvested 3 days after injection with plasmids and dsRNA. Gene expression was normalized by *rp49* and expressed as $2^{-\text{dCt}}$ values.

* $p < 0.05$; ** $p < 0.01$; *** $p < 0.001$ (Student's t test). Data are from the same experiment shown in panel (B).

validity of the reporter assay. Finally, we observed that the silencing of Firefly *luciferase* was maintained upon co-transfection with the dsRNA targeting *TSN*, suggesting that *TSN* does not enhance RNAi function in *Ae. aegypti* (Figure 5B). We measured expression levels of *TSN* and *Ago2* upon co-transfection with reporter plasmids and dsRNA and verified that *TSN* and *Ago2* expression levels were significantly reduced upon knockdown with their specific dsRNA (Figures 5C and 5D). Although we cannot exclude that residual *TSN* expression could suffice to maintain its activity, the knockdown efficiency was similar to that of *Ago2*. Overall, these results supported the conclusion that *TSN* is not a positive regulator of RNAi in *Ae. aegypti*. One caveat of this RNAi reporter assay is that we could only reliably assess a positive effect of *TSN* on RNAi activity (i.e., measure higher luminescence counts). Indeed, the efficiency of *luciferase* silencing was very high in the presence of dsRNA, which may have prevented our ability to detect a negative effect of *TSN* knockdown on RNAi activity (i.e., lower luminescence counts than the dsLuc + dsGFP control).

Small RNA Profiling in *TSN*-Depleted Mosquitoes

To overcome the limitations inherent to the RNAi reporter assay, and further assess the impact of *TSN* depletion on RNAi activity, we deep sequenced small RNA populations in *TSN*-depleted mosquitoes infected with DENV-1. We first injected adult mosquitoes with dsRNA targeting *TSN* or *luciferase* as a control. Two days later, we exposed mosquitoes to DENV-1 via an infectious blood meal. Four days after exposure to the virus, we performed a second injection of dsRNA against *TSN* and *luciferase* to prolong gene silencing (Figure 6A). We verified *TSN* knockdown by measuring *TSN* expression levels on days 4 and 10 post infection (Figures S3A, related to Figure 6). We then selected mosquitoes that were infected with

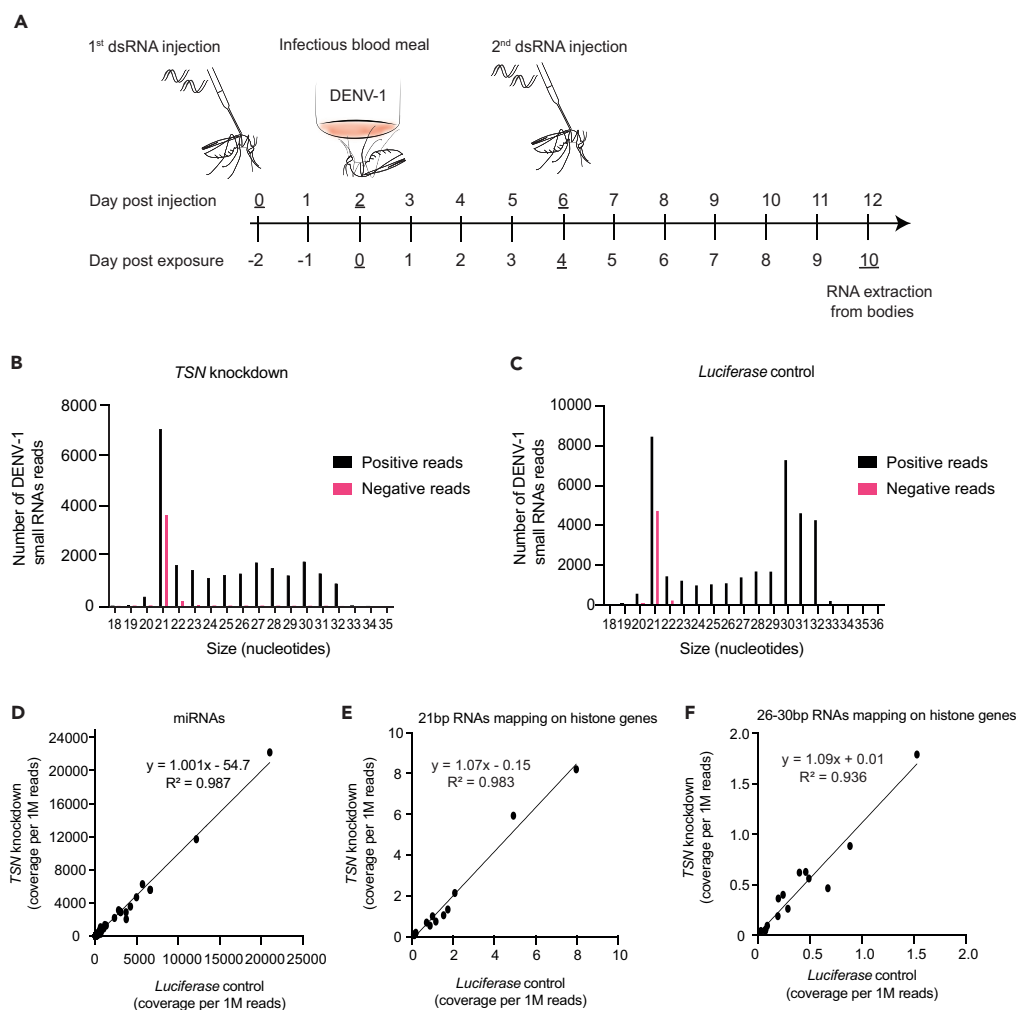


Figure 6. Small RNA Populations Are Unchanged Following TSN Knockdown

(A) Experimental scheme. Adult female mosquitoes were injected with dsRNA targeting *luciferase* or *TSN* 2 days before and 4 days after a DENV-1 infectious blood meal. Whole bodies were harvested on day 10 post infection for RNA extraction and deep sequencing of small RNAs.

(B and C) Size distribution of the total number of DENV-1-specific small RNA reads normalized to the total number of reads upon (B) *TSN* knockdown or (C) *luciferase* control.

(D–F) Linear relationship between the amount of viral and cellular small RNAs in *TSN* knockdown versus *luciferase* control mosquitoes 10 days post DENV-1 infection. Data points represent the normalized number of reads (coverage per 1M reads) corresponding to (D) miRNAs, (E) endo-siRNAs mapping on histone coding sequences, and (F) endo-piRNAs mapping on histone coding sequences. For miRNAs, each dot represents one miRNA. For siRNAs and piRNAs mapping on histone genes, each dot represents a histone gene. For siRNAs and piRNAs mapping on the DENV-1 sequence, each dot represents a 500-bp region of the viral genome. Lines represent the linear regression of each set of values. The equation and R^2 value of each regression are shown next to the line.

See also Figure S3.

DENV-1 and displayed low *TSN* expression for sequencing, as well as control mosquitoes injected with dsRNA targeting *luciferase* that had equivalent DENV-1 RNA levels but normal *TSN* expression (Figure S3B, related to Figure 6). These mosquitoes were used to prepare and sequence small RNA libraries and compare the three canonical small RNA populations: miRNAs, siRNAs (21 nucleotides in length), and piRNAs (26–30 nucleotides in length). We first examined small RNAs mapping on the DENV-1 genome. As expected, 21-nucleotide (nt)-long siRNAs were highly abundant in both the *TSN*-depleted mosquitoes (Figure 6B) and control mosquitoes (Figure 6C), and they were distributed across the viral genome, on both strands, in both conditions (Figures S3C and S3D, related to Figure 6). Next, we examined small RNAs

mapping on the mosquito genome. We found that *TSN* depletion did not affect the miRNA machinery, as miRNA abundance was very similar between both conditions tested (Figure 6D). Likewise, we found that *TSN* knockdown did not influence siRNA and piRNA biogenesis. The abundance of both histone-derived siRNAs (Figure 6E) and histone-derived piRNAs (Figure 6F) was similar between the *TSN*-depleted mosquitoes and controls.

DISCUSSION

Antiviral immunity in *Ae. aegypti* mosquitoes remains poorly understood. Using a novel approach of transcriptomic analysis, we previously uncovered four genes that not only responded to DENV infection in the mosquito midgut but also had expression levels that correlated with viral loads in infected mosquitoes (Raquin et al., 2017). Here, we focused on one of these four genes, *Tudor-SN*, encoding a member of the Tudor protein family. *TSN* was induced upon DENV-1 infection, and its expression correlated positively with viral RNA load (Raquin et al., 2017). Using RNAi-mediated knockdown assays *in vivo* and *in vitro*, we demonstrated that *TSN* promotes both DENV-1 and DENV-3 replication. *TSN* knockdown also resulted in a slight decrease of CHIKV replication, but it was not statistically significant. We performed localization studies and discovered that *TSN* localizes to the nucleolus of *Ae. aegypti* and *Ae. albopictus* cells and does not colocalize with DENV-1 replication sites. Moreover, we found that, despite belonging to the Tudor family, *TSN* was not essential for RNAi function in adult mosquitoes.

TSN is a known component of the RISC, the RNAi protein complex that carries siRNAs and directs cleavage of complementary viral sequences in *Caenorhabditis elegans*, *Drosophila*, and mammals (Caudy et al., 2003). Additionally, previous work in *Drosophila* and other model organisms found essential functions for Tudor domain-containing proteins in piRNA biogenesis. A recent study describing a functional knockdown screen of all predicted *Ae. aegypti* Tudor proteins did not reveal a role for Tudor-SN in piRNA biogenesis (Joosten et al., 2019). This finding is consistent with our observations that Tudor-SN is not necessary for the piRNA pathway function *in vivo* in *Ae. aegypti*. Finally, Tudor-SN was also shown to be a conserved component of the basic RNAi machinery in *Ixodes* ticks (Ayllon et al., 2015). This study reported an effect of Tudor-SN on dsRNA-mediated gene silencing, which possibly involves the siRNA pathway. However, no evidence was obtained for a role of Tudor-SN in the response to microbial infection (Ayllon et al., 2015). Taken together, the data described in this study and discussed above did not find strong links between RNAi function and Tudor-SN in arthropods. Further studies using knockout mutants might be necessary to confirm these findings.

The mammalian ortholog of Tudor-SN is generally referred to as p100 and was identified as a host factor interacting with the 3' untranslated region of the DENV genome (Lei et al., 2011). Moreover, p100 knockdown led to reduced levels of viral RNA and protein in mammalian cells, providing evidence that p100 was required for efficient DENV replication. Although these results are consistent with those reported here, in mammalian cells p100 was shown to interact with DENV genomic RNA and dsRNA replication intermediates, which we did not observe. Importantly, the subcellular localization of p100 in mammalian cells was perinuclear, whereas it was nucleolar in mosquito cells. This discrepancy in localization hints to a divergence in function between mammals, in which p100 interacts directly with viral RNA, and insects, for which evidence is lacking. Microscopy-based localization studies being limited in sensitivity and resolution, elucidating Tudor-SN function in mosquitoes will require further experiments to more definitely exclude interactions between viral RNA and Tudor-SN, such as protein immunoprecipitation and sequencing of associated RNA (RIP-seq).

The predicted structure of *Ae. aegypti* Tudor-SN includes four Staphylococcal Nuclease (SN)-like domains and a Tudor domain embedded in a fifth SN domain. Tudor-SN homologs are found in diverse eukaryotic species such as plants, humans (Staphylococcal Nuclease and Tudor domain containing 1), and insects (*Drosophila* Tudor-SN). The very similar structure of eukaryotic Tudor-SN homologs is consistent with potentially conserved functions (Figure 7). However, Tudor-SN subcellular localization is variable in other species, which also hints toward species-specific function(s) of Tudor-SN proteins.

Our observation that *Ae. aegypti* Tudor-SN localizes primarily to the nucleolus of mosquito cells makes it unlikely that its proviral effect on DENV relies on a direct action on viral genome stability or replication. The nucleolus is a multifunctional nuclear domain involved in ribosome biogenesis and several other cellular functions, such as cell cycle regulation, telomere metabolism, or DNA damage sensing and repair (Lam and Trinkle-Mulcahy, 2015). Various nucleolar alterations during viral infection have been documented (Salvetti and Greco,

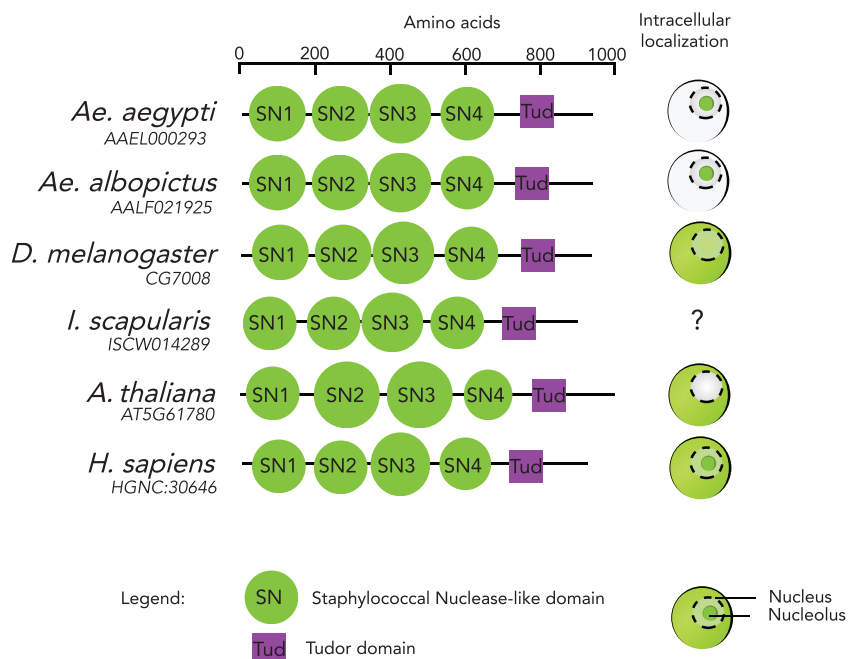


Figure 7. Conserved Structure of TSN Homologs Among Diverse Eukaryotic Species

Structural domains provided in the UniProt database are shown for homologs of *Ae. aegypti* TSN (Q17PM3) in *Drosophila melanogaster* (Q9W0S7), *Ixodes scapularis* (B7QIP4), *Arabidopsis thaliana* (F4K6N0), and *Homo sapiens* (Q7KZF4). Diagrams on the right side indicate TSN subcellular localization (in green) in the cytoplasm, nucleus, and/or nucleolus of each species based on the literature (Fashe et al., 2013; Ku et al., 2016; Gutierrez-Beltran et al., 2015; Frei dit Frey et al., 2010; Caudy et al., 2003).

2014). Interestingly, DENV non-structural protein 5 (NS5), which encodes the virus RNA-dependent RNA polymerase, was recently shown to localize to the nucleolus of infected mammalian cells (Fraser et al., 2016), where it interferes with precursor messenger RNAs (pre-mRNA) splicing to limit host antiviral response (De Maio et al., 2016). Human Tudor-SN was implicated in spliceosome assembly and, therefore, may influence splicing of pre-mRNAs and/or interact with DENV NS5 to facilitate viral RNA accumulation (Gao et al., 2012). More generally, Tudor-SN could promote viral replication through regulation of gene expression. For example, the Jak-Stat pathway protects *Ae. aegypti* against DENV infection (Souza-Neto et al., 2009) and Tudor-SN was shown to bind Stat proteins to modulate host gene transcription (Pauku and Silvennoinen, 2004). Also, Tudor-SN is a component of stress granules (Gao et al., 2014) and could interfere with their formation to facilitate DENV infection (Miller, 2011). Particularly interesting is the early proviral effect of TSN in the mosquito midgut, which might suggest a role for TSN in viral sensing, or early antiviral responses. For instance, TSN might sense the infection and, in the nucleus, alter the spliceosome to increase the availability of cellular resources that the virus requires to replicate. Its presence in the nucleolus and at the nucleus-nucleolus interface might enhance ribosome biogenesis and subsequently increase production of viral proteins.

Although several pathways involved in antiviral immunity have been characterized in mosquitoes, several aspects of anti-DENV defense remain to be elucidated, particularly during the early phase of infection. For example, the siRNA pathway was recently shown to inefficiently restrict DENV replication in the *Ae. aegypti* midgut (Olmo et al., 2018). The present work adds to the small number of studies that identified DENV proviral factors in mosquitoes (Londono-Renteria et al., 2015; Jupatanakul et al., 2014; Sessions et al., 2009; Raquin et al., 2017). Such host factors have been proposed as new targets for antiviral therapy in humans (Savidis et al., 2016; Zhang et al., 2016; Marceau et al., 2016). Although the development of novel vector control methods has focused on viral restriction factors so far (Flores and O'neill, 2018), targeting essential host factors could complement antiviral strategies in mosquitoes. We showed that Tudor-SN is such a host factor for DENV in the mosquito *Ae. aegypti*. Further studies will be necessary to elucidate the specific mechanisms underlying the role of Tudor-SN in DENV replication.

Limitations of the Study

We demonstrated a proviral role of *TSN* upon DENV infection in the mosquito midgut. Our study primarily relied on gene knockdown to diminish *TSN* expression *in vitro* and *in vivo*, and it will be useful in the future to confirm the results using knockout mosquitoes. Second, this study used a strain of *Ae. aegypti* from Thailand, and it remains to be determined whether the proviral role of *TSN* extends to other mosquito strains. Finally, additional in-depth functional studies are required to elucidate the exact role of *TSN*.

METHODS

All methods can be found in the accompanying [Transparent Methods supplemental file](#).

DATA AND CODE AVAILABILITY

The accession number for the RNA-seq data set reported in this paper is SRA: PRJNA386455.

SUPPLEMENTAL INFORMATION

Supplemental Information can be found online at <https://doi.org/10.1016/j.isci.2020.100870>.

ACKNOWLEDGMENTS

We thank Lambrechts and Saleh lab members, Marie-Agnès Dillies, and two anonymous reviewers for helpful comments and discussions. We are grateful to Catherine Lallemand for assistance with mosquito rearing and to Davy Jiolle and Christophe Paupy for providing the DENV-3 isolate. We thank Alongkot Ponlawat for the initial field sampling of mosquitoes in Thailand. We thank Alain Kohl for sharing the reporter plasmids and Emilie Pondeville for her insights on the reporter assay protocol. This work was supported by the Institut Pasteur Transversal Research Program (grant PTR-410 to L.L. and M.-C.S.), the French Government's Investissement d'Avenir program, Laboratoire d'Excellence Integrative Biology of Emerging Infectious Diseases (grant ANR-10-LABX-62-IBEID to L.L. and M.-C.S.), the City of Paris Emergence(s) program in Biomedical Research (to L.L.), the European Research Council (grant FP7/2013-2019 ERC CoG 615220 to M.-C.S.), and the European Union's Horizon 2020 research and innovation program under ZikaPLAN grant agreement no. 734584 (to L.L.). The funders had no role in study design, data collection and analysis, decision to publish, or preparation of the manuscript.

AUTHOR CONTRIBUTIONS

S.H.M., V.R., S.D., M.-C.S., and L.L. designed the experiments; S.H.M., V.R., S.D., I.M.-C., A.H.-L., and H.B. performed the experiments; S.H.M., V.R., H.V., L.F., and L.L. analyzed the data; S.H.M., V.R., M.-C.S., and L.L. wrote the paper.

DECLARATION OF INTERESTS

The authors declare no competing interests.

Received: August 29, 2019

Revised: December 24, 2019

Accepted: January 24, 2020

Published: February 21, 2020

REFERENCES

- Ayllon, N., Naranjo, V., Hajdusek, O., Villar, M., Galindo, R.C., Kocan, K.M., Alberdi, P., Sima, R., Cabezas-Cruz, A., Ruckert, C., et al. (2015). Nuclease tudor-SN is involved in tick dsRNA-mediated RNA interference and feeding but not in defense against flaviviral or anaplasma phagocytophilum rickettsial infection. *PLoS One* 10, e0133038.
- Bartholomay, L.C., and Michel, K. (2018). Mosquito immunobiology: the intersection of vector health and vector competence. *Annu. Rev. Entomol.* 63, 145–167.
- Bhatt, S., Gething, P.W., Brady, O.J., Messina, J.P., Farlow, A.W., Moyes, C.L., Drake, J.M., Brownstein, J.S., Hoen, A.G., Sankoh, O., et al. (2013). The global distribution and burden of dengue. *Nature* 496, 504–507.
- Black, W.C.T., Bennett, K.E., Gorrochotegui-Escalante, N., Barillas-Mury, C.V., Fernandez-Salas, I., De Lourdes Munoz, M., Farfan-Ale, J.A., Olson, K.E., and Beaty, B.J. (2002). Flavivirus susceptibility in *Aedes aegypti*. *Arch. Med. Res.* 33, 379–388.
- Brady, O.J., Gething, P.W., Bhatt, S., Messina, J.P., Brownstein, J.S., Hoen, A.G., Moyes, C.L., Farlow, A.W., Scott, T.W., and Hay, S.I. (2012). Refining the global spatial limits of dengue virus transmission by evidence-based consensus. *PLoS Negl. Trop. Dis.* 6, e1760.
- Campbell, C.L., Keene, K.M., Brackney, D.E., Olson, K.E., Blair, C.D., Wilusz, J., and Foy, B.D. (2008). *Aedes aegypti* uses RNA interference in defense against Sindbis virus infection. *BMC Microbiol.* 8, 47.

- Caudy, A.A., Ketting, R.F., Hammond, S.M., Denli, A.M., Bathoorn, A.M., Tops, B.B., Silva, J.M., Myers, M.M., Hannon, G.J., and Plasterk, R.H. (2003). A micrococcal nuclease homologue in RNAi effector complexes. *Nature* 425, 411–414.
- Champer, J., Buchman, A., and Akbari, O.S. (2016). Cheating evolution: engineering gene drives to manipulate the fate of wild populations. *Nat. Rev. Genet.* 17, 146–159.
- De Maio, F.A., Risso, G., Iglesias, N.G., Shah, P., Pozzi, B., Gebhard, L.G., Mammi, P., Mancini, E., Yanovsky, M.J., Andino, R., et al. (2016). The dengue virus NS5 protein intrudes in the cellular spliceosome and modulates splicing. *PLoS Pathog.* 12, e1005841.
- Emara, M.M., and Brinton, M.A. (2007). Interaction of TIA-1/TIAR with West Nile and dengue virus products in infected cells interferes with stress granule formation and processing body assembly. *Proc. Natl. Acad. Sci. U S A* 104, 9041–9046.
- Fashe, T., Saarikettu, J., Isomaki, P., Yang, J., and Silvennoinen, O. (2013). Expression analysis of Tudor-SN protein in mouse tissues. *Tissue Cell* 45, 21–31.
- Flores, H.A., and O’neill, S.L. (2018). Controlling vector-borne diseases by releasing modified mosquitoes. *Nat. Rev. Microbiol.* 16, 508–518.
- Fontaine, A., Jiolle, D., Moltini-Conclois, I., Lequime, S., and Lambrechts, L. (2016). Excretion of dengue virus RNA by *Aedes aegypti* allows non-destructive monitoring of viral dissemination in individual mosquitoes. *Sci. Rep.* 6, 24885.
- Franz, A.W., Sanchez-Vargas, I., Adelman, Z.N., Blair, C.D., Beaty, B.J., James, A.A., and Olson, K.E. (2006). Engineering RNA interference-based resistance to dengue virus type 2 in genetically modified *Aedes aegypti*. *Proc. Natl. Acad. Sci. U S A* 103, 4198–4203.
- Fraser, J.E., Rawlinson, S.M., Heaton, S.M., and Jans, D.A. (2016). Dynamic nucleolar targeting of dengue virus polymerase NS5 in response to extracellular pH. *J. Virol.* 90, 5797–5807.
- Frei Dit Frey, N., Muller, P., Jammes, F., Kizis, D., Leung, J., Perrot-Rechenmann, C., and Bianchi, M.W. (2010). The RNA binding protein Tudor-SN is essential for stress tolerance and stabilizes levels of stress-responsive mRNAs encoding secreted proteins in *Arabidopsis*. *Plant Cell* 22, 1575–1591.
- Gao, X., Shi, X., Fu, X., Ge, L., Zhang, Y., Su, C., Yang, X., Silvennoinen, O., Yao, Z., He, J., et al. (2014). Human Tudor staphylococcal nuclease (Tudor-SN) protein modulates the kinetics of AGTR1-3’UTR granule formation. *FEBS Lett.* 588, 2154–2161.
- Gao, X., Zhao, X., Zhu, Y., He, J., Shao, J., Su, C., Zhang, Y., Zhang, W., Saarikettu, J., Silvennoinen, O., et al. (2012). Tudor staphylococcal nuclease (Tudor-SN) participates in small ribonucleoprotein (snRNP) assembly via interacting with symmetrically dimethylated Sm proteins. *J. Biol. Chem.* 287, 18130–18141.
- Gentile, C., Lima, J.B., and Peixoto, A.A. (2005). Isolation of a fragment homologous to the rp49 constitutive gene of *Drosophila* in the Neotropical malaria vector *Anopheles aquasalis* (Diptera: Culicidae). *Mem. Inst. Oswaldo Cruz.* 100, 545–547.
- Gould, E., Pettersson, J., Higgs, S., Charrel, R., and De Lamballerie, X. (2017). Emerging arboviruses: why today? *One Health* 4, 1–13.
- Gutierrez-Beltran, E., Moschou, P.N., Smertenko, A.P., and Bozhkov, P.V. (2015). Tudor staphylococcal nuclease links formation of stress granules and processing bodies with mRNA catabolism in *Arabidopsis*. *Plant Cell* 27, 926–943.
- Joosten, J., Miesen, P., Taskopru, E., Pennings, B., Jansen, P., Huynen, M.A., Vermeulen, M., and Van Rij, R.P. (2019). The Tudor protein Veneno assembles the ping-pong amplification complex that produces viral piRNAs in *Aedes* mosquitoes. *Nucleic Acids Res.* 47, 2546–2559.
- Jupatanakul, N., Sim, S., and Dimopoulos, G. (2014). *Aedes aegypti* ML and Niemann-Pick type C family members are agonists of dengue virus infection. *Dev. Comp. Immunol.* 43, 1–9.
- Katzelnick, L.C., Fonville, J.M., Gromowski, G.D., Bustos Arriaga, J., Green, A., James, S.L., Lau, L., Montoya, M., Wang, C., Vanblargan, L.A., et al. (2015). Dengue viruses cluster antigenically but not as discrete serotypes. *Science* 349, 1338–1343.
- Keene, K.M., Foy, B.D., Sanchez-Vargas, I., Beaty, B.J., Blair, C.D., and Olson, K.E. (2004). RNA interference acts as a natural antiviral response to O’nyong-nyong virus (Alphavirus; Togaviridae) infection of *Anopheles gambiae*. *Proc. Natl. Acad. Sci. U S A* 101, 17240–17245.
- Ku, H.Y., Gangaraju, V.K., Qi, H., Liu, N., and Lin, H. (2016). Tudor-SN interacts with piwi antagonistically in regulating spermatogenesis but synergistically in silencing transposons in *Drosophila*. *PLoS Genet.* 12, e1005813.
- Lam, Y.W., and Trinkle-Mulcahy, L. (2015). New insights into nucleolar structure and function. *F1000prime Rep.* 7, 48.
- Lasko, P. (2010). Tudor domain. *Curr. Biol.* 20, R666–R667.
- Lee, W.S., Webster, J.A., Madzokere, E.T., Stephenson, E.B., and Herrero, L.J. (2019). Mosquito antiviral defense mechanisms: a delicate balance between innate immunity and persistent viral infection. *Parasit. Vectors* 12, 165.
- Lei, Y., Huang, Y., Zhang, H., Yu, L., Zhang, M., and Dayton, A. (2011). Functional interaction between cellular p100 and the dengue virus 3’ UTR. *J. Gen. Virol.* 92, 796–806.
- Londono-Renteria, B., Troupin, A., Conway, M.J., Vesely, D., Ledizet, M., Roundy, C.M., Cloherty, E., Jameson, S., Vanlandingham, D., Higgs, S., et al. (2015). Dengue virus infection of *Aedes aegypti* requires a putative cysteine rich venom protein. *PLoS Pathog.* 11, e1005202.
- Marceau, C.D., Puschnik, A.S., Majzoub, K., Ooi, Y.S., Brewer, S.M., Fuchs, G., Swaminathan, K., Mata, M.A., Elias, J.E., Sarnow, P., and Carette, J.E. (2016). Genetic dissection of Flaviviridae host factors through genome-scale CRISPR screens. *Nature* 535, 159–163.
- Merkling, S.H., Bronkhorst, A.W., Kramer, J.M., Overheul, G.J., Schenck, A., and Van Rij, R.P. (2015a). The epigenetic regulator g9a mediates tolerance to RNA virus infection in *Drosophila*. *PLoS Pathog.* 11, e1004692.
- Merkling, S.H., Overheul, G.J., Van Mierlo, J.T., Arends, D., Gilissen, C., and Van Rij, R.P. (2015b). The heat shock response restricts virus infection in *Drosophila*. *Sci. Rep.* 5, 12758.
- Merkling, S.H., and Van Rij, R.P. (2013). Beyond RNAi: antiviral defense strategies in *Drosophila* and mosquito. *J. Insect Physiol.* 59, 159–170.
- Messina, J.P., Brady, O.J., Golding, N., Kraemer, M.U.G., Wint, G.R.W., Ray, S.E., Pigott, D.M., Shearer, F.M., Johnson, K., Earl, L., et al. (2019). The current and future global distribution and population at risk of dengue. *Nat. Microbiol.* 4, 1508–1515.
- Miesen, P., Joosten, J., and Van Rij, R.P. (2016). PIWIs go viral: arbovirus-derived piRNAs in vector mosquitoes. *PLoS Pathog.* 12, e1006017.
- Miller, C.L. (2011). Stress granules and virus replication. *Future Virol.* 6, 1329–1338.
- Mongelli, V., and Saleh, M.C. (2016). Bugs are not to be silenced: small RNA pathways and antiviral responses in insects. *Annu. Rev. Virol.* 3, 573–589.
- Myles, K.M., Wiley, M.R., Morazzani, E.M., and Adelman, Z.N. (2008). Alphavirus-derived small RNAs modulate pathogenesis in disease vector mosquitoes. *Proc. Natl. Acad. Sci. U S A* 105, 19938–19943.
- Olmo, R.P., Ferreira, A.G.A., Izidoro-Toledo, T.C., Aguiar, E., de Faria, I.J.S., de Souza, K.P.R., Osorio, K.P., Kuhn, L., Hammann, P., de Andrade, et al. (2018). Control of dengue virus in the midgut of *Aedes aegypti* by ectopic expression of the dsRNA-binding protein Loqs2. *Nat. Microbiol.* 3, 1385–1393.
- Pastorino, B., Bessaud, M., Grandadam, M., Murri, S., Tolou, H.J., and Peyrefitte, C.N. (2005). Development of a TaqMan® RT-PCR assay without RNA extraction step for the detection and quantification of African Chikungunya viruses. *J. Virol. Methods* 124, 65–71.
- Pauku, K., and Silvennoinen, O. (2004). STATs as critical mediators of signal transduction and transcription: lessons learned from STAT5. *Cytokine Growth Factor Rev.* 15, 435–455.
- Raquin, V., and Lambrechts, L. (2017). Dengue virus replicates and accumulates in *Aedes aegypti* salivary glands. *Virology* 507, 75–81.
- Raquin, V., Merklings, S.H., Gausson, V., Moltini-Conclois, I., Frangeul, L., Varet, H., Dillies, M.A., Saleh, M.C., and Lambrechts, L. (2017). Individual co-variation between viral RNA load and gene expression reveals novel host factors during early dengue virus infection of the *Aedes aegypti* midgut. *PLoS Negl. Trop. Dis.* 11, e0006152.
- Salazar, M.I., Richardson, J.H., Sanchez-Vargas, I., Olson, K.E., and Beaty, B.J. (2007). Dengue virus type 2: replication and tropisms in orally infected *Aedes aegypti* mosquitoes. *BMC Microbiol.* 7, 9.
- Salvetti, A., and Greco, A. (2014). Viruses and the nucleolus: the fatal attraction. *Biochim. Biophys. Acta* 1842, 840–847.

Sanchez-Vargas, I., Scott, J.C., Poole-Smith, B.K., Franz, A.W., Barbosa-Solomieu, V., Wilusz, J., Olson, K.E., and Blair, C.D. (2009). Dengue virus type 2 infections of *Aedes aegypti* are modulated by the mosquito's RNA interference pathway. *PLoS Pathog.* 5, e1000299.

Savidis, G., Mcdougall, W.M., Meraner, P., Perreira, J.M., Portmann, J.M., Trincucci, G., John, S.P., Aker, A.M., Renzette, N., Robbins, D.R., et al. (2016). Identification of Zika virus and dengue virus dependency factors using functional genomics. *Cell Rep.* 16, 232–246.

Sessions, O.M., Barrows, N.J., Souza-Neto, J.A., Robinson, T.J., Hershey, C.L., Rodgers, M.A., Ramirez, J.L., Dimopoulos, G., Yang, P.L., Pearson, J.L., and Garcia-Blanco, M.A. (2009). Discovery of insect and human dengue virus host factors. *Nature* 458, 1047–1050.

Sigle, L.T., and McGraw, E.A. (2019). Expanding the canon: non-classical mosquito genes at the interface of arboviral infection. *Insect Biochem. Mol. Biol.* 109, 72–80.

Simoes, M.L., Caragata, E.P., and Dimopoulos, G. (2018). Diverse host and restriction factors regulate mosquito-pathogen interactions. *Trends Parasitol.* 34, 603–616.

Siomi, M.C., Mannen, T., and Siomi, H. (2010). How does the royal family of Tudor rule the PIWI-interacting RNA pathway? *Genes Dev.* 24, 636–646.

Sirri, V., Urcuqui-Inchima, S., Roussel, P., and Hernandez-Verdun, D. (2008). Nucleolus: the fascinating nuclear body. *Histochem. Cell Biol.* 129, 13–31.

Souza-Neto, J.A., Sim, S., and Dimopoulos, G. (2009). An evolutionary conserved function of the JAK-STAT pathway in anti-dengue defense. *Proc. Natl. Acad. Sci. U S A* 106, 17841–17846.

Van Cleef, K.W., Van Mierlo, J.T., Van Den Beek, M., and Van Rij, R.P. (2011). Identification of viral suppressors of RNAi by a reporter assay in *Drosophila* S2 cell culture. *Methods Mol. Biol.* 721, 201–213.

Weaver, S.C. (2013). Urbanization and geographic expansion of zoonotic arboviral diseases: mechanisms and potential strategies for prevention. *Trends Microbiol.* 21, 360–363.

Weber, F., Wagner, V., Rasmussen, S.B., Hartmann, R., and Paludan, S.R. (2006). Double-stranded RNA is produced by positive-strand RNA viruses and DNA viruses but not in detectable amounts by negative-strand RNA viruses. *J. Virol.* 80, 5059–5064.

Yakob, L., Funk, S., Camacho, A., Brady, O., and Edmunds, W.J. (2017). *Aedes aegypti* control through modernized, integrated vector management. *PLoS Curr.* 9, <https://doi.org/10.1371/currents.outbreaks.45deb8e03a438c4d088afb4fafaee8747>.

Zhang, R., Miner, J.J., Gorman, M.J., Rausch, K., Ramage, H., White, J.P., Zuiani, A., Zhang, P., Fernandez, E., Zhang, Q., et al. (2016). A CRISPR screen defines a signal peptide processing pathway required by flaviviruses. *Nature* 535, 164–168.

iScience, Volume 23

Supplemental Information

Tudor-SN Promotes Early Replication of Dengue Virus in the *Aedes aegypti* Midgut

Sarah Hélène Merklings, Vincent Raquin, Stéphanie Dabo, Annabelle Henrion-Lacritick, Hervé Blanc, Isabelle Moltini-Conclois, Lionel Frangeul, Hugo Varet, Maria-Carla Saleh, and Louis Lambrechts

Supplementary figure legends

Supplementary Figure 1. *TSN* is transiently upregulated in the midgut following a blood meal, related to Figure 3. *TSN* expression levels on day 1 (A) and day 4 (B) in the midgut, head, ovary, abdomen, and thorax in sugar-fed mosquitoes (control) or following a non-infectious blood meal. *TSN* expression was normalized by *rp49* and expressed as $2^{-\text{dCt}}$ value. Organs were collected in pools of 10 and tested in triplicates. *P* values above the graph indicate statistical significance assessed with a Wilcoxon test.

Supplementary Figure 2. *TSN* promotes DENV-3 infection but not CHIKV infection in the mosquito midgut, related to Figure 3. (A, C, E) *TSN* expression levels and (B) DENV-3 or (D, F) CHIKV RNA levels following gene knockdown on day 2 (C, D), and day 4 (A, B, E, F) after an infectious blood meal. Mean percentages of gene expression knockdown are indicated. *TSN* expression was normalized by *rp49* and expressed as $2^{-\text{dCt}}$ values in $n = 20-24$ individual mosquito midguts per group. *P* values above the graph indicate statistical significance assessed with a Wilcoxon test.

Supplementary Figure 3. *TSN* knockdown does not significantly affect the coverage of siRNAs mapping on the DENV-1 genome, related to Figure 6. *TSN* expression levels (A) and DENV-1 viral RNA levels (B) on day 4 and 10 post blood meal in whole adult mosquitoes injected with dsRNA targeting *luciferase* or *TSN*. *TSN* expression and viral levels were normalized by *rp49* and expressed as $2^{-\text{dCt}}$ values in $n = 17-32$ individual mosquitoes per group. *P* values above the graph indicate statistical significance assessed with a Wilcoxon test. Colored dots represent mosquitoes selected for the small RNA sequencing. The normalized coverage of 21-nt reads mapping on the positive and negative viral strands is shown across the DENV-1 genome for the (C) *luciferase* control and (D) *TSN* knockdown conditions.

Transparent methods

Ethics

The Institut Pasteur animal facility has received accreditation from the French Ministry of Agriculture to perform experiments on live animals in compliance with the French and European regulations on care and protection of laboratory animals. This study was approved by the Institutional Animal Care and Use Committee at Institut Pasteur under protocol number 2015–0032.

Cells and virus

C6/36 cells (derived from *Ae. albopictus*) and Aag2 cells (derived from *Ae. aegypti*) were cultured in Leibovitz's L-15 medium (Life Technologies) supplemented with 10% fetal bovine serum (FBS, Life Technologies), 1% non-essential amino acids (Life Technologies) and 0.1% Penicillin-Streptomycin (Life Technologies) at 28°C. DENV type 1 (DENV-1) isolate KDH0030A was originally derived in 2010 from the serum of a dengue patient at the Kamphaeng Phet Provincial Hospital, Thailand (Fansiri et al., 2013). The full-length consensus genome sequence is available from GenBank under accession number GenBank: HG316482. DENV-3 isolate GA28-7 was originally derived in 2010 from the serum of a dengue patient in Moanda, Gabon (Caron et al., 2013). CHIKV isolate M105 (Caribbean strain) was described previously (Stapleford et al., 2016) and its genome sequence is available from GenBank under accession number GenBank: LN898104.1. Viral stocks were prepared in C6/36 cells for DENV and Vero cells (ATCC CRL-1586) for CHIKV. Infectious titers of DENV were measured on C6/36 cells using a standard focus-forming assay (FFA) (Fontaine et al., 2016), and infectious titers of CHIKV were measured on Vero cells using a standard plaque assay (Goic et al., 2016).

Mosquito rearing and experimental infections

All experiments were performed with adult *Ae. aegypti* mosquitoes derived from a field population originally sampled in 2013 in Thep Na Korn, Kamphaeng Phet Province, Thailand. Experiments took place within 16 generations of laboratory colonization. Mosquitoes were reared in standard insectary conditions, as previously reported (Fontaine et al., 2016). Experimental virus infections were performed in a level-3 containment facility, as previously described (Fontaine et al., 2016). Shortly, 5- to 7-day-old female mosquitoes were deprived of

10% sugar solution 24h before oral exposure to viruses. The infectious blood meal consisted of a 2:1 mix of washed rabbit erythrocytes and viral suspension (to reach an infectious titer of 10^7 FFU/mL) supplemented with 10 mM ATP (Sigma). Mosquitoes were fed for 30 min through a pig-intestine membrane using an artificial feeder (Hemotek Ltd) set at 37°C. Fully engorged females were incubated at 28°C, 70% relative humidity and under a 12-hour light-dark cycle with permanent access to 10% sucrose till further use.

RNA isolation from mosquito midguts

Midguts were dissected in 1x PBS, and immediately transferred to a tube containing 800 μ L of Trizol (Life Technologies) and ~20 1-mm glass beads (BioSpec). Samples were homogenized for 30 sec at 6,000 rpm in a Precellys 24 grinder (Bertin Technologies). RNA was extracted as previously described (Raquin et al., 2017), and stored at -80°C till further use.

Reverse transcription and quantitative PCR

Viral RNA was reverse transcribed and quantified using a TaqMan based qPCR assay, using NS5-specific primers and 6-FAM/BHQ-1 double-labeled probe (sequences provided in Table 1). Reactions were performed with the Superscript III Platinum One-Step qRT-PCR kit (Life technologies) following the manufacturer's instructions and as previously described (Fontaine et al., 2016). The limit of detection of the assay was 10 copies of viral RNA per μ L. *Tudor-SN* and *Ago2* expression levels were measured using a SybrGreen based qPCR assay, using gene-specific primers (sequences provided in Table 1). First, total RNA from individual midguts or adults was reverse transcribed into cDNA using MMLV reverse transcriptase (Invitrogen), according to manufacturer's instructions. Quantitative PCR was performed on a LightCycler 96 real-time thermocycler (Roche) using SYBR Green MasterMix from Roche (Figure 3) or Promega (Figures 2, 5, S1, S2, S3). qPCR efficiency and Ct values were unaffected by change of SYBR Green reagent. The qPCR programs was as follows: an initial denaturation step of 5 min at 95°C, followed by 40 cycles of 10 sec at 95°C, 20 sec at 60°C and 10 sec at 72°C. A melting curve was generated to confirm the absence of non-specific PCR amplicons using the following program: 5 sec at 95°C, 60 sec at 65°C and continuous fluorescence acquisition up to 97°C with a ramp rate 0.2°C/sec. Relative expression was calculated as $2^{-((Cq_{rp49} - Cq_{gene}))}$, using the *Ae. aegypti* ribosomal protein-coding gene *rp49* (AAEL003396) for normalization.

Double-stranded RNA synthesis

Design and synthesis of dsRNA used in knockdown assays has been described previously (Raquin et al., 2017). Briefly, dsRNA was synthesized from a GFP-containing plasmid or from a cDNA template produced by RT-PCR on RNA isolated from a pool of *Ae. aegypti* mosquitoes. T7 promoter sequences were incorporated by PCR to the amplicon that was used as a template for the synthesis using the MEGAscript RNAi kit (Life Technologies).

Gene silencing assays *in vivo*

RNAi-mediated knockdown of target genes was performed as previously described (Raquin et al., 2017). Briefly, 500 ng of dsRNA targeting Firefly *luciferase* (*FLuc*), and 1 μ g of dsRNA targeting *TSN*, *Ago2* or *GFP* was injected intra-thoracically using Nanoject II or III (Drummond). Injection volume was 140 nL except for the RNAi reporter assay described below. Control mosquitoes were injected with a dsRNA targeting Green Fluorescent Protein (GFP). After injection, mosquitoes were incubated for 3 days at 28°C before exposure to an infectious blood meal.

RNAi reporter assay

RNAi competency of adult mosquitoes was assed using a reporter assay adapted from previously published methods in *Drosophila* (Merkling et al., 2015a; Merklng et al., 2015b; van Cleef et al., 2011). *In vivo* plasmid transfection method was optimized from protocols previously published for *Ae. aegypti* (Colpitts et al., 2011; Isoe et al., 2007). Five to seven-day-old adult mosquitoes were injected in the thorax using a Nanoject III (Drummond) with a suspension of \approx 300 nL containing a 1:1 mixture of unsupplemented Leibovitz's L-15 medium (Life technologies) and Cellfectin II (Thermo Fisher Scientific) complexed with 50 ng pUb-GL3 (encoding Firefly *luciferase*, FLuc), 50 ng pCMV-RLuc (encoding Renilla *luciferase*) described previously (Anderson et al., 2010; Varjak et al., 2017), and 500 ng FLuc-specific and 1 μ g *GFP*-, *TSN*- or *Ago2*-specific dsRNA. After incubation for 3 days at 28°C, mosquitoes were homogenized in passive lysis buffer (Promega) using the Precellys 24 grinder (Bertin Technologies) for 30 sec at 6,000 rpm. Samples were transferred to a 96-well plate and centrifugated for 5 min at 12000 x g. Fifty microliters of supernatant were transferred to a new plate, and 50 μ L LARII reagent added for the first FLuc measurement. Next, 50 μ L Stop&Glow

reagent was added before the second measurement of RLuc, according to the Dual Luciferase assay reporter system (Promega). Counts of RLuc were used to control for transfection efficiency, and samples with less than 1,000 counts were discarded from the analysis. Data were normalized by calculating the ratio Fluc/RLuc.

Immunofluorescence assays

Mock- and DENV-1-infected Aag2 cells were fixed on coverslips using 4% paraformaldehyde (Sigma-Aldrich) for 30 min at room temperature (20-25°C). Following permeabilization with 1X PBS, 0.1% Triton-X100, cells were incubated with mouse anti-dsRNA α K1 (English & Scientific consulting) and rabbit anti-TSN antibodies diluted 1:500 in 1X PBS, 0.1% Triton-X100, 2% Normal Goat Serum for 1 hour at room temperature. Subsequently, cells were washed three times with 1X PBS with 0.1% Triton X-100 and incubated with goat anti-mouse AlexaFluor 594 and goat anti-rabbit Alexa Fluor 488 diluted 1:1.000 in 1X PBS, 0.1% Triton-X100, 2% Normal Goat Serum (Life technologies), overnight at 4°C. After three washes in 1X PBS with 0.1% Triton X-100, cover slips were mounted on a glass slide in ~10 μ L Prolong Gold anti-fade medium containing DAPI (Thermo Fisher) and imaged with a confocal microscope LSM 700 inverted (Zeiss) at 63X magnification.

Gene silencing and DENV-1 infection *in vitro*

Aag2 cells were transfected in 24-well plates with 500 ng of dsRNA using Lipofectamine LTX (Invitrogen) along with Plus reagent according to the manufacturer's instructions. To increase knockdown efficiency, a second round of transfection with 500 ng of dsRNA was performed 48 hours after the initial transfection. Infection with DENV-1 was performed 24 hours after the last transfection. Cells were incubated for 1 hour in L-15 infection medium containing 2% FBS and DENV-1 at a multiplicity of infection of 1. After removal of the infectious inoculum, cells were refreshed with fully supplemented with L-15 medium and incubated at 28°C.

Western blotting

Aag2 cells were harvested, washed once in PBS and resuspended in RIPA buffer (20 mM Hepes-KOH pH 7.5, 100 mM KCl, 5% glycerol, 0.05% NP40, with freshly added 0.1M DTT and complete, EDTA-free, protease inhibitors (Roche)). Cells were lysed in Laemelli buffer (Sigma-Aldrich) with 10% β -mercaptoethanol and incubated at 95°C for 5 min. Protein lysates were

loaded on a 4–20% precast mini-protean polyacrylamide gel (Bio-Rad) then transferred to a nitrocellulose membrane. The blot was incubated for 1 hr at room temperature with rabbit anti-TSN antibody (Abcam 65078) diluted 1:200 in blocking buffer (5% skimmed milk powder, 0.1% Triton-X100 in 1X PBS). After 3 washes with 1X PBS, the blot was incubated with a secondary antibody, HRP-conjugated polyclonal goat anti-rabbit IgG (GE Healthcare) diluted 1:5.000 in 1X PBS, 0.1% Triton-X100 for 1 hour at room temperature. Next, the blot was incubated with a primary anti- β -actin murine antibody (Sigma-Aldrich, clone AC-74) at 1:6.000 dilution in blocking buffer, and an HRP-conjugated polyclonal goat anti-mouse IgG (GE Healthcare) diluted at 1:5.000 in 1X PBS, 0.1% Triton-X100 was used as a secondary antibody. Bound antibodies were revealed by chemiluminescence with the SuperSignal West Pico Chemiluminescent Substrate (Fisher Scientific). Quantification of band intensities was performed in ImageJ (Davarinejad, 2017).

Small RNA libraries

Total RNA from pools of 2 (dsLuc) or 3 (dsTSN) whole mosquitoes was isolated with TRIzol (Invitrogen). Small RNAs of 19-33 nucleotides in length were purified from a 15% acrylamide/bisacrylamide (37.5:1), 7 M urea gel as described previously (Gausson and Saleh, 2011). Purified RNAs were used for library preparation using the NEBNext Multiplex Small RNA Library Prep kit for Illumina (E7300 L) with the 3' adaptor from IDT (linker 1) and in-house designed indexed primers. Libraries were diluted to 4 nM and sequenced using an Illumina NextSeq 500 High Output kit v2 (75 cycles) on an Illumina NextSeq 500 platform. Sequence reads were analyzed with in-house Perl scripts.

Bioinformatics analysis of small RNA libraries

The quality of fastq files was assessed using graphs generated by 'FastQC' (<http://www.bioinformatics.babraham.ac.uk/projects/fastqc/>). Quality and adaptors were trimmed from each read using 'cutadapt' (<https://code.google.com/p/cutadapt/>). Only reads with acceptable quality (phred score ≥ 20) were retained. A second set of graphs was generated by 'FastQC' (<http://www.bioinformatics.babraham.ac.uk/projects/fastqc/>) on the fastq files created by 'cutadapt' (Martin, 2011). Mapping was performed by 'Bowtie1' (Langmead et al., 2009) with the '-v 1' option (one mismatch between the read and its target). 'Bowtie1' generates results in 'sam' format. All 'sam' files were analyzed by different tools of the package 'samtools' (Li et al., 2009) to produce 'bam' indexed files. To analyze these 'bam'

files, different kind of graphs were generated using home-made R scripts with several Bioconductor libraries such as 'Rsamtools' or 'Shortreads' (<http://bioconductor.org/>).

Statistical analysis

Statistical analysis methods have been described previously (Raquin et al., 2017). Additionally, statistical significance tests as implanted in GraphPad Prism version 7. *P* values below 0.05 were considered statistically significant.

Supplementary references

Anderson, M.A., Gross, T.L., Myles, K.M., and Adelman, Z.N. (2010). Validation of novel promoter sequences derived from two endogenous ubiquitin genes in transgenic *Aedes aegypti*. *Insect Mol Biol* *19*, 441-449.

Caron, M., Grard, G., Paupy, C., Mombo, I.M., Bikie Bi Nso, B., Kassa Kassa, F.R., Nkoghe, D., and Leroy, E.M. (2013). First evidence of simultaneous circulation of three different dengue virus serotypes in Africa. *PLoS ONE* *8*, e78030.

Colpitts, T.M., Cox, J., Vanlandingham, D.L., Feitosa, F.M., Cheng, G., Kurscheid, S., Wang, P., Krishnan, M.N., Higgs, S., and Fikrig, E. (2011). Alterations in the *Aedes aegypti* transcriptome during infection with West Nile, dengue and yellow fever viruses. *PLoS Pathog* *7*, e1002189.

Davarinejad, H. (2017). Quantifications of western blots with Image J. <https://di.uq.edu.au/community-and-alumni/sparq-ed/sparq-ed-services/using-imagej-quantify-blots>

Fansiri, T., Fontaine, A., Diancourt, L., Caro, V., Thaisomboonsuk, B., Richardson, J.H., Jarman, R.G., Ponlawat, A., and Lambrechts, L. (2013). Genetic mapping of specific interactions between *Aedes aegypti* mosquitoes and dengue viruses. *PLoS Genet* *9*, e1003621.

Fontaine, A., Jiolle, D., Moltini-Conclois, I., Lequime, S., and Lambrechts, L. (2016). Excretion of dengue virus RNA by *Aedes aegypti* allows non-destructive monitoring of viral dissemination in individual mosquitoes. *Sci Rep* *6*, 24885.

Gausson, V., and Saleh, M.C. (2011). Viral small RNA cloning and sequencing. *Methods Mol Biol* *721*, 107-122.

Goic, B., Stapleford, K.A., Frangeul, L., Doucet, A.J., Gausson, V., Blanc, H., Schemmel-Jofre, N., Cristofari, G., Lambrechts, L., Vignuzzi, M., *et al.* (2016). Virus-derived DNA drives mosquito vector tolerance to arboviral infection. *Nat Commun* 7, 12410.

Isoe, J., Kunz, S., Manhart, C., Wells, M.A., and Miesfeld, R.L. (2007). Regulated expression of microinjected DNA in adult *Aedes aegypti* mosquitoes. *Insect Mol Biol* 16, 83-92.

Langmead, B., Trapnell, C., Pop, M., and Salzberg, S.L. (2009). Ultrafast and memory-efficient alignment of short DNA sequences to the human genome. *Genome Biol* 10, R25.

Li, H., Handsaker, B., Wysoker, A., Fennell, T., Ruan, J., Homer, N., Marth, G., Abecasis, G., Durbin, R., and Genome Project Data Processing, S. (2009). The Sequence Alignment/Map format and SAMtools. *Bioinformatics* 25, 2078-2079.

Martin, M. (2011). Cutadapt removes adapter sequences from high-throughput sequencing reads. *EMBnet Journal*, 17, 10-12.

Merkling, S.H., Bronkhorst, A.W., Kramer, J.M., Overheul, G.J., Schenck, A., and Van Rij, R.P. (2015a). The epigenetic regulator g9a mediates tolerance to RNA virus infection in *Drosophila*. *PLoS Pathog* 11, e1004692.

Merkling, S.H., Overheul, G.J., van Mierlo, J.T., Arends, D., Gilissen, C., and van Rij, R.P. (2015b). The heat shock response restricts virus infection in *Drosophila*. *Sci Rep* 5, 12758.

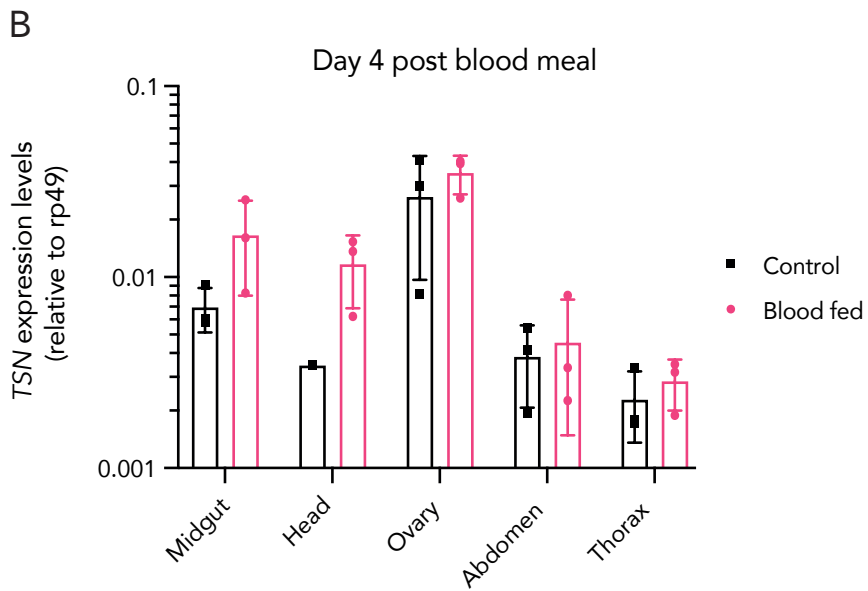
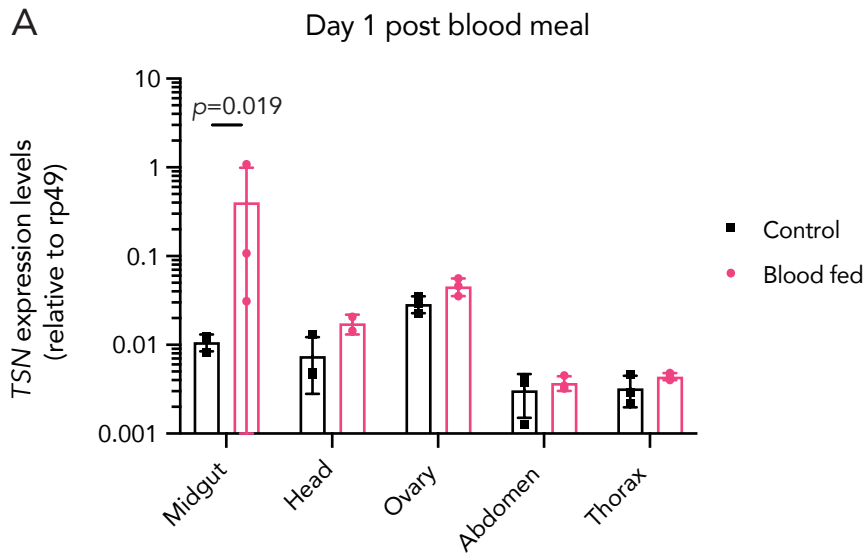
Raquin, V., Merklings, S.H., Gausson, V., Moltini-Conclois, I., Frangeul, L., Varet, H., Dillies, M.A., Saleh, M.C., and Lambrechts, L. (2017). Individual co-variation between viral RNA load and gene expression reveals novel host factors during early dengue virus infection of the *Aedes aegypti* midgut. *PLoS Negl Trop Dis* 11, e0006152.

Stapleford, K.A., Moratorio, G., Henningsson, R., Chen, R., Matheus, S., Enfissi, A., Weissglas-Volkov, D., Isakov, O., Blanc, H., Mounce, B.C., *et al.* (2016). Whole-Genome Sequencing Analysis from the Chikungunya Virus Caribbean Outbreak Reveals Novel Evolutionary Genomic Elements. *PLoS Negl Trop Dis* 10, e0004402.

van Cleef, K.W., van Mierlo, J.T., van den Beek, M., and van Rij, R.P. (2011). Identification of viral suppressors of RNAi by a reporter assay in *Drosophila* S2 cell culture. *Methods Mol Biol* 721, 201-213.

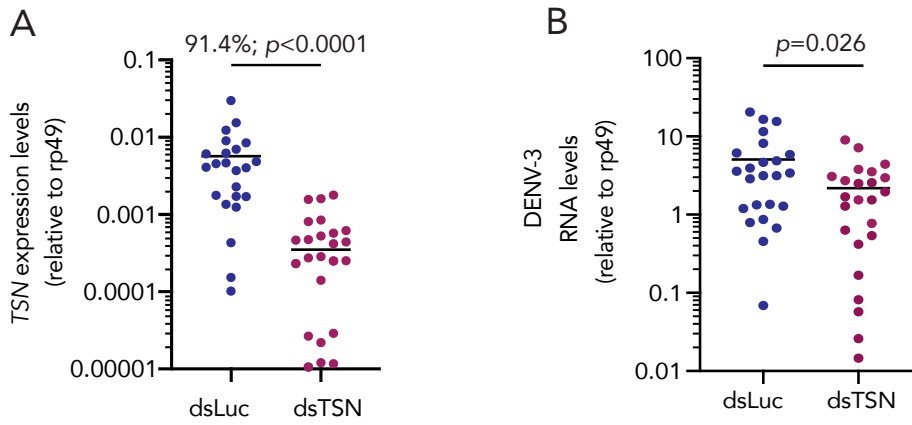
Varjak, M., Maringer, K., Watson, M., Sreenu, V.B., Fredericks, A.C., Pondeville, E., Donald, C.L., Sterk, J., Kean, J., Vazeille, M., *et al.* (2017). *Aedes aegypti* Piwi4 Is a Noncanonical PIWI Protein Involved in Antiviral Responses. *mSphere* 2.

Supplementary figure 1

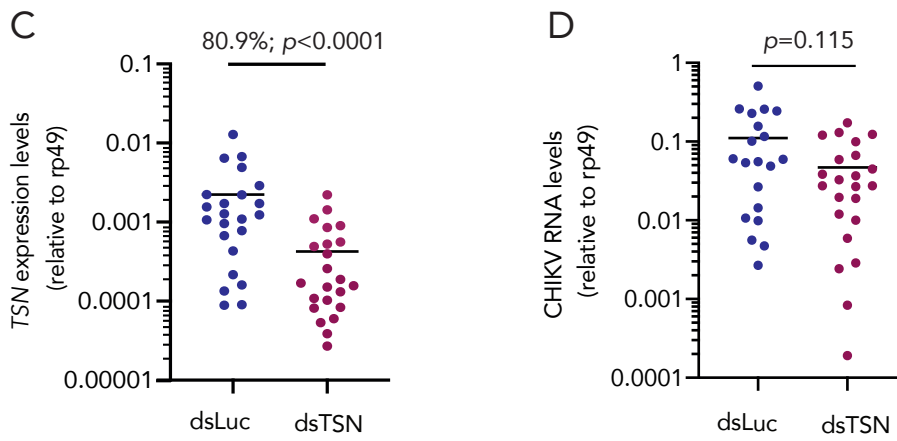


Supplementary figure 2

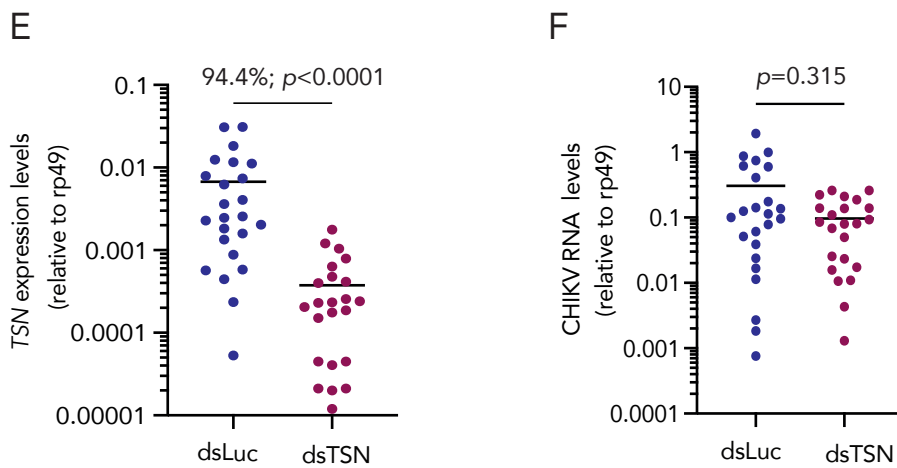
DENV-3 - Day 4 post infection



CHIKV - Day 2 post infection



CHIKV - Day 4 post infection



Supplementary figure 3

